

**NASA TECHNICAL
MEMORANDUM**

NASA TM X- 72662
COPY NO.

NASA TM X- 72662

**THEORETICAL PERFORMANCE OF CROSS-WIND AXIS TURBINES
WITH RESULTS FOR A CATENARY VERTICAL AXIS CONFIGURATION**

By

Ralph J. Muraca, Maria V. Stephens and J. Ray Dagenhart

**Langley Research Center
Hampton, Virginia**



This informal documentation medium is used to provide accelerated or special release of technical information to selected users. The contents may not meet NASA formal editing and publication standards, may be revised, or may be incorporated in another publication.

**NATIONAL AERONAUTICS AND SPACE ADMINISTRATION
LANGLEY RESEARCH CENTER, HAMPTON, VIRGINIA 23665**

**(NASA-TM-X-72662) THEORETICAL PERFORMANCE
OF CROSS-WIND AXIS TURBINES WITH RESULTS FOR
A CATENARY VERTICAL AXIS CONFIGURATION
(NASA) 85 p HC \$5.00**

N76-11032

CSCL 01A

Unclass

G3/02 01571

1. Report No. NASA TM X-72662		2. Government Accession No.		3. Recipient's Catalog No.	
4. Title and Subtitle Theoretical Performance of Cross-Wind Axis Turbines with Results for a Catenary Vertical Axis Configuration.				5. Report Date OCTOBER 1975	
				6. Performing Organization Code	
7. Author(s) Ralph J. Muraca, Maria V. Stephens, and J. Ray Dagenhart				8. Performing Organization Report No.	
9. Performing Organization Name and Address NASA/Langley Research Center Hampton, VA 23665				10. Work Unit No. 501-06-01-01	
				11. Contract or Grant No.	
12. Sponsoring Agency Name and Address National Aeronautics and Space Administration Washington, DC 20546				13. Type of Report and Period Covered Technical Memorandum	
				14. Sponsoring Agency Code	
15. Supplementary Notes					
16. Abstract <p>A general analysis capable of predicting performance characteristics of cross-wind axis turbines has been developed. This analysis includes the effects of airfoil geometry, support struts, blade aspect ratio, windmill solidity, blade interference and curved flow. The results from the analysis are compared with available wind tunnel results for a catenary blade shape. A theoretical performance curve for an aerodynamically efficient straight blade configuration is also presented. In addition, a linearized analytical solution applicable for straight blade configurations is developed. A listing of the computer program developed for numerical solutions of the general performance equations is included in the appendix.</p>					
17. Key Words (Suggested by Author(s)) (STAR category underlined) cross-wind axis turbine, vertical axis windmill, windmill performance, Darrieus rotor,				18. Distribution Statement Unclassified - Unlimited	
19. Security Classif. (of this report) Unclassified		20. Security Classif. (of this page) Unclassified		21. No. of Pages 85	
				22. Price* \$4.75	

**THEORETICAL PERFORMANCE OF CROSS-WIND AXIS TURBINES
WITH RESULTS FOR A CATENARY VERTICAL AXIS CONFIGURATION**

TMX - 72662

By .

**Ralph J. Muraca
Maria V. Stephens
J. Ray Dagenhart**

SUMMARY

A general analysis capable of predicting performance characteristics of vertical axis windmills (VAW) has been developed. This analysis includes the effects of airfoil geometry, support struts, blade aspect ratio, windmill solidity, blade interference and curved flow. The results from the analysis are compared with available wind tunnel results for a catenary blade shape. A theoretical performance curve for an aerodynamically efficient straight blade configuration is also presented. In addition, a linearized analytical solution applicable for straight blade configurations is developed. This analysis is useful for parameter studies when the aerodynamic characteristics of the airfoil can be assumed to behave linearly with angle of attack. The errors introduced by this assumption are demonstrated by comparing numerical with analytical results. A listing of the computer program developed for numerical solutions of the general performance equations is included in the appendix.

SYMBOLS

AR	aspect ratio
A_s	swept or projected area in vertical plane
a	lift curve slope for two dimensional airfoil
C_D	drag coefficient
C_L	lift coefficient
C_M	moment coefficient
C_{M_a}	coefficient of the average moment produced during one revolution of the windmill
C_P	power coefficient
C_p	pressure coefficient
C_{p_L}	pressure coefficient - lower surface
C_{p_U}	pressure coefficient - upper surface
C_T	thrust coefficient
c	chord length
D	drag
x	chordwise distance from airfoil leading edge to center of pressure
h	height of windmill
K_1	lift curve slope including aspect ratio and downwash corrections
L	lift
l	length
M	moment

SYMBOLS CONTINUED

N	normal force
n	number of blades
P	power
P_t	total wind stream power
q	dynamic pressure
R	tip speed to wind speed ratio
Re_y	Reynolds number
r	distance from axis of rotation to half chord point of blade element
r'	distance from axis of rotation to any particular point along blade chord line
s	spanwise distance
T_h	thrust
V	wind speed at windmill
V_r	wind speed relative to blades
V_∞	wind speed in free stream
x	chordwise distance from leading edge
y	vertical distance
α	angle of attack
β	local blade slope angle
ϵ	angle in plane of rotation between r and r' directions
θ	angle of rotation from wind direction
ξ	chordwise distance from half chord point forward
ρ_∞	air density
ω	rotational speed

SYMBOLS CONTINUED

Subscripts:

\bar{a}	average
m, \max	maximum
r	relative
T	total
0	reference
∞	free stream

Superscripts:

$—$	nondimensional
\cdot	time derivative

INTRODUCTION

As a consequence of the current shortages of fossil fuels interest is being revived in alternate sources of energy. One means for converting solar energy to a more useful form is through the use of windmills. Windmills may take many forms from drag devices to those which utilize the efficiency of airfoil shapes. An interesting survey of various types of windmills is given in reference 1. The most common windmill using airfoil shapes is the conventional multibladed horizontal axis type. These range from two blades to as high as twenty-seven blades depending on application, and the blades may range from propeller type to flexible sails. Analyses of horizontal axis windmills are well documented.

Another category of windmill is the vertical axis (VAW) or Darrieus windmill. The primary attraction of a VAW is the simplicity of manufacture compared to a HAW, and the manner in which the loads developed during operation are resisted by the structure. These differences indicate that if the efficiency of a VAW is equal to or not much less than a conventional windmill, use of a VAW might result in a more economical energy conversion system.

In recent years a small body of data has been published on the vertical axis windmill. Some of these reports present the results from tests of the vertical axis concept, ref. 2 and 3, while others present various analyses, structural, aerodynamic,

and economic, of vertical axis windmills, references 4 through 7.

This report presents a general analysis of vertical axis windmills. Airfoil theory is used to determine the torque generated by the blades about the axis of rotation, and momentum theory is used to determine the effective wind velocity at the blades. These yield a set of integral equations which require an iterative approach for their solution. The nonlinear characteristics of the blade airfoils are accounted for in the general analysis. A more simplified analysis assuming linear aerodynamics and applicable to straight blade configuration is also presented.

The results of this analysis in addition to being in good agreement with available test data on one VAW concept indicate that the VAW can be designed such that their efficiency is comparable to the best horizontal axis designs.

This report presents the details of the general nonlinear analysis and the linearized analytical solutions for the straight blade concept. The results produced from the general analysis are compared with existing test data. The results from a parameter study of VAW's using the general analysis and the linearized solutions are compared and limitations of the linear analysis are identified. One straight blade configuration having significantly improved aerodynamic performance while maintaining the same structural capability of the tested configuration is also analyzed and the results are presented. Also included in the Appendix of

this report is a listing, of a computer program for general analyses of vertical axis windmills along with input and results for a sample case.

GENERAL THEORY

In this section, general nondimensional equations for aerodynamic torque and average windmill thrust are developed by use of actuator disk theory and blade element aerodynamics. Real effects such as aspect ratio, downwash and flow curvature are accounted for. An average nondimensional power coefficient is defined and its relation to wind speed and average windmill torque is given.

Defining Equations

The basic elements of the vertical axis windmill are shown on figure 1. It is composed of an arbitrary number of blades (the figures are shown with two) attached to a rotating shaft which is nominally perpendicular to free stream velocity vector. The blades shown in the figure are straight; however, this is not a requirement. The blade cross section must be such that when subjected to an angle of attack a lift force is generated. The performance of the windmill is directly related to the ratio of this lift force to the blade drag. Since the angle of attack which the blades experience is cyclic the blade cross sections are restricted to symmetric shapes.

The coordinate system used in this analysis is shown in figure 2. The origin is located at the midpoint of the rotor with the y axis corresponding to the spin axis. The wind velocity is arbitrarily assumed to be directed along the x-axis. The rotor position as given by the angle θ is measured from the x-axis. The local radius is measured

from the y-axis and the local slope, β , is measured with respect to the radius vector.

The determination of local lift and drag characteristics of a blade element represents an unsteady flow problem. However, it has been assumed that the static aerodynamic data for the subject airfoil section is applicable.

Consider an arbitrary blade section as shown in figure 3. For a blade element the incremental forces acting in radial and tangential directions are derived as follows. The total velocity at any location on a blade is,

$$V_r^2 = (r\omega - V \sin \theta)^2 + (V \cos \theta)^2 \quad (1)$$

The angle of attack is given by

$$\tan \alpha = \frac{V \cos \theta \sin \beta}{r\omega - V \sin \theta} \quad (2)$$

The incremental forces developed as a consequence of the angle of attack are defined as, dL , in the direction normal to the relative velocity vector, and dD , in the direction of the relative velocity.

These forces act to produce a moment about the axis of rotation given by

$$dM = (dL \sin \alpha - dD \cos \alpha) r + (dL \cos \alpha + dD \sin \alpha) \sin \beta \left(\frac{C}{2} - d \right) \quad (3)$$

The elemental lift and drag force can be written as

$$dL = C_L q c ds \quad (4a)$$

and

$$dD = C_D q c ds \quad (4b)$$

where the element length, ds , is given by $ds = dy/\sin \beta$.

Substituting eq. (4) into eq. (3) yields

$$dM = (C_L q c(dy/\sin \beta) \sin \alpha - C_D q c(dy/\sin \beta) \cos \alpha) r \\ + (C_L q c(dy/\sin \beta) \cos \alpha + C_D q c(dy/\sin \beta) \sin \alpha) \sin \beta \left(\frac{c}{2} - d\right), \quad (5)$$

where $q = \frac{1}{2} \rho_\infty V_r^2$.

Integrating over y yields the total moment due to the blade as a function of the angle θ .

$$M(\theta) = \int_{-h/2}^{h/2} (C_L \sin \alpha - C_D \cos \alpha) \frac{r q c dy}{\sin \beta} \\ + \int_{-h/2}^{h/2} (C_L \cos \alpha + C_D \sin \alpha) q c \left(\frac{c}{2} - d\right) dy \quad (6)$$

The following nondimensionalization scheme is used; all velocities are nondimensionalized using the free stream velocity, V_∞ , and all lengths are nondimensionalized using the maximum radius of the windmill blades r_{\max} . The nondimensional variables are denoted by a bar, i.e. $\bar{V} = V/V_\infty$. With this notation equation (6) becomes,

$$M(\theta) = \frac{1}{2} \rho_\infty V_\infty^2 (r_{\max})^3 \int_{-\bar{h}/2}^{\bar{h}/2} (C_L \sin \alpha - C_D \cos \alpha) \frac{\bar{r} \bar{c} \bar{V}_r^2 d\bar{y}}{\sin \beta} \\ + \frac{1}{2} \rho_\infty V_\infty^2 (r_{\max})^3 \int_{-\bar{h}/2}^{\bar{h}/2} (C_L \cos \alpha + C_D \sin \alpha) \bar{V}_r^2 \bar{c} \left(\frac{\bar{c}}{2} - \bar{d}\right) d\bar{y} \quad (7)$$

If a moment coefficient, C_M , is defined as

$$C_M \equiv \frac{M}{\frac{1}{2} \rho_{\infty} V_{\infty}^2 r_{\max}^3 \bar{A}_s} \quad (8)$$

where \bar{A}_s is the area swept out by the windmill then eq. (7) becomes

$$C_M(\theta) = \frac{1}{\bar{A}_s} \int_{-\bar{h}/2}^{\bar{h}/2} [(C_L \sin \alpha - C_D \cos \alpha) \frac{\bar{r}}{\sin \beta} + (C_L \cos \alpha + C_D \sin \alpha) (\frac{\bar{c}}{2} - \bar{d})] \bar{c} \bar{v}_r^2 d\bar{y}$$

This can be rewritten as

$$C_M(\theta) = \frac{2}{\bar{A}_s} \int_0^{\bar{h}/2} \frac{\bar{c} \bar{r} \bar{v}_r^2}{\sin \beta} [(C_L \sin \alpha - C_D \cos \alpha) + \frac{\bar{c}}{\bar{r}} (\frac{1}{2} - \frac{\bar{d}}{\bar{c}}) \sin \beta (C_L \cos \alpha + C_D \sin \alpha)] d\bar{y} \quad (9)$$

Equation (9) holds for one blade, if there are n blades in the configuration the contribution for each blade can be obtained by replacing θ in equations (1) and (2) by $\theta + (i-1) \Delta\theta$ and re-evaluating equation (9).

Doing this the total moment coefficient can be written

$$C_{M_T}(\theta) = \sum_{i=1}^{i=n} C_{M_i}(\theta + (i-1) \Delta\theta) \quad (10)$$

where $\Delta\theta = \frac{2\pi}{n}$.

The integral of the total moment through one revolution of the windmill is given by

$$C_{M_N} = n \int_0^{2\pi/n} C_{M_T}(\theta) d\theta \quad (11)$$

The average moment is then given by

$$C_{M_a} = \frac{C_{M_N}}{2\pi} = \frac{n}{2\pi} \int_0^{2\pi/n} C_{M_T}(\theta) d\theta \quad (12)$$

The average power developed by the windmill is given by

$$P = \frac{\omega n}{2\pi} \int_0^{2\pi/n} M_T(\theta) d\theta \quad (13)$$

Defining a power coefficient C_p as

$$C_p = \frac{P}{P_t}$$

where

$$P_t = \frac{1}{2} \dot{m} V_\infty^2 = \frac{1}{2} \rho_\infty A_s V_\infty^3$$

represents the total kinetic energy available per unit time in the stream tube. Using the definition of eq. (9), eq. (13) can be written in terms of the average moment coefficient as

$$P = \frac{1}{2} \rho_{\infty} (V_{\infty}^2) A_s C_{M_a} (r_{\max}) \quad (14)$$

thereby giving

$$C_P = \left(\frac{r_{\max}}{V_{\infty}} \right) C_{M_a}$$

or

$$C_P = R C_{M_a} \quad (15)$$

where

$$R \equiv \left(\frac{r_{\max}}{V_{\infty}} \right)$$

In nondimensional form equations (1) and (2) become

$$\bar{V}_r^2 = (R \bar{r} - \bar{V} \sin \theta)^2 + \bar{V}^2 \cos^2 \theta \quad (16)$$

and

$$\tan \alpha = \frac{\bar{V} \cos \theta \sin \beta}{\bar{r} R - \bar{V} \sin \theta} \quad (17)$$

Momentum Loss and Windmill Thrust

The thrust acting on any device extracting energy from the wind is directly related to the change in momentum which occurs in the wind stream. Using momentum theory, reference 8 gives

$$T_h = 2 \rho_\infty \bar{V} (1 - \bar{V}) A_s V_\infty^2 \quad (18)$$

or

$$C_{T_a} = 4 \bar{V} (1 - \bar{V})$$

where C_{T_a} is an average thrust coefficient and is defined as

$$C_{T_a} \equiv \frac{T_h}{\frac{1}{2} \rho_\infty V_\infty^2 A_s} \quad (19)$$

In terms of the elemental forces acting on a blade section the average thrust coefficient can be written

$$C_{T_a} = \frac{n}{2\pi} \int_0^{2\pi/n} \frac{2\bar{c}}{\bar{A}_s} \int_{-\bar{h}/2}^{\bar{h}/2} \frac{\bar{V}^2}{\sin \beta} [(C_L \cos \alpha + C_D \sin \alpha) \cos \theta \sin \beta + (C_L \sin \alpha - C_D \cos \alpha) \sin \theta] d\bar{y} d\theta \quad (20)$$

The determination of C_{T_a} and \bar{V} for specified values of V_∞ requires an iterative procedure.

Real Effects

Although determining the flow field around a rotating windmill airfoil constitutes a 3 dimensional unsteady flow problem, the assumption has been made in this analysis that the flow is steady and that a two dimensional analysis can be used. However, a number of other effects including aspect ratio, downwash and curved flow can influence the rotor performance and some attempt has been made to evaluate these.

Aspect Ratio. - During a rotation through 360 degrees a blade section will experience large angles of attack as the ratio of rw/V_{∞} becomes small. When this occurs blade stall will result and to account for stall effects, it is necessary to use experimental data on section lift, drag and moment coefficients. These data are generally presented for infinite aspect ratio wings with appropriate aspect ratio correction being required. From reference 9 using Prandtl's lifting line theory, aspect ratio correction can be written as

$$C_L = C_{L_o} / (1 + \frac{a_o}{\pi AR}) \quad (21a)$$

and

$$C_D = C_{D_o} + \frac{C_L^2}{\pi AR} \quad (21b)$$

where C_{L_o} & C_{D_o} represents the lift and drag coefficient for an infinite aspect ratio wing, and $AR = h/c$.

Downwash. - For a multibladed configuration each blade is in the downwash from the preceding blade thus the angle of attack is reduced by

this downwash angle. Again using the approach outlined in reference 9 the effect of downwash can be accounted for by using an aspect ratio correction. This yields

$$C_L = C_{L_0} \left[\frac{1 - a_0 / \pi AR}{1 + a_0 / \pi AR} \right] . \quad (22)$$

Flow Curvature. - Since the airfoil is traveling in a circular arc the angle of attack varies along the length of the chord. The effect of flow curvature is a function of the spin rate and the chord to radius ratio. This effect can be evaluated by considering the flow over a flat plate. The force distribution on a plate of unit width in a uniform stream of velocity V_∞ , is given by

$$\frac{dN}{dx} = q (C_{p_L} - C_{p_U}) \quad (23)$$

For a flat plate the velocity ratio at angle of attack is given by reference 10 as

$$\frac{V}{V_\infty} = \cos \alpha \pm \sin \alpha \left(\frac{c - x}{x} \right), \quad (24)$$

where the (+) and (-) signs refer to the upper and lower surfaces, respectively. Now the relation between V/V_∞ and C_p is

$$C_p = 1 - (V/V_\infty)^2 \quad (25)$$

Substituting yields

$$\frac{dN}{dx} = 4 q \cos \alpha \sin \alpha \left(\frac{c - x}{x} \right) \quad (26)$$

Since the blade is actually moving along a curved path, the local angle of attack will vary. Referring to figure 4 the local angle of attack

can be written as

$$\cot \alpha = \frac{r'\omega \cos \varepsilon - V_{\infty} \sin \theta}{V_{\infty} \cos \theta - r'\omega \sin \varepsilon}$$

or

$$\cot \alpha = \frac{r\omega - V_{\infty} \sin \theta}{V_{\infty} \cos \theta - \xi \omega}$$

or

$$\cot \alpha = \frac{R - \sin \theta}{\cos \theta - \xi R} \quad (27)$$

where $R = r\omega/V_{\infty}$.

In terms of the coordinate \bar{x} measured from the leading edge of the plate this becomes

$$\cot \alpha = \frac{R - \sin \theta}{\cos \theta + R(\bar{x} - \bar{c}/2)} \quad (28)$$

In terms of the lift distribution on the plate eq. (26) becomes

$$\frac{dL}{d\bar{x}} = 4 q \cos^2 \alpha \sin \alpha \left(\frac{\bar{c} - \bar{x}}{\bar{x}} \right) \quad (29)$$

In the limiting case $\bar{c} \rightarrow 0$ and the expression for angle of attack becomes

$$\cot \alpha_0 = \frac{R - \sin \theta}{\cos \theta}.$$

Defining a reference lift distribution as

$$\left(\frac{dL}{d\bar{x}} \right)_0 = 4 q \cos^2 \alpha_0 \sin \alpha_0 \left(\frac{\bar{c} - \bar{x}}{\bar{x}} \right)$$

the effect of curvature can be displayed as a function of the ratio of lift distributions, with and without curvature effects. That is

$$\frac{(dL/d\bar{x})}{(dL/d\bar{x})_0} = \frac{\cos^2 \alpha \sin \alpha}{\cos^2 \alpha_0 \sin \alpha_0} \quad (30)$$

The ratio of lift with and without curvature effects can be written

$$\frac{L}{L_0} = \frac{\int_0^{\bar{c}} \cos^2 \alpha \sin \alpha d\bar{x}}{\int_0^{\bar{c}} \cos^2 \alpha_0 \sin \alpha_0 d\bar{x}} = \frac{\int_0^{\bar{c}} \cos^2 \alpha \sin \alpha d\bar{x}}{\cos^2 \alpha_0 \sin \alpha_0 \bar{c}} \quad (31)$$

The numerator can be integrated giving

$$\frac{L}{L_0} = \frac{\frac{R - \sin \theta}{R} (\cos \alpha_1 - \cos \alpha_2)}{\cos^2 \alpha_0 \sin \alpha_0 \bar{c}} \quad (32)$$

where

$$\begin{aligned} \alpha_0 &= \tan^{-1} \left(\frac{\cos \theta}{R - \sin \theta} \right) \\ \alpha_1 &= \tan^{-1} \left(\frac{\cos \theta - \frac{R \bar{c}}{2}}{R - \sin \theta} \right) \\ \alpha_2 &= \tan^{-1} \left(\frac{\cos \theta + \frac{R \bar{c}}{2}}{R - \sin \theta} \right) \end{aligned}$$

This correction term has been applied to account for flow curvature effects. For most typical configurations the correction is less than one percent. However, if \bar{c} becomes large this effect would become more important.

VERIFICATION OF GENERAL THEORY

In this section, the difficulties of modeling windmill performance using airfoil data with corrections for three dimensional flow effects are discussed. Theoretical results are compared to test data.

Reynolds Number, Roughness and Crossflow

As indicated in reference 11 the NACA 0012 airfoil falls into the category which experiences either leading edge or trailing edge stall depending on Reynolds Number.

Furthermore, the section characteristics are very dependent on surface roughness. When these effects are combined with the three dimensional nature of the flow over the windmill blades it becomes apparent that using two dimensional data at a fixed Reynolds Number represents a significant approximation.

Fortunately, use of two dimensional data yields a good approximation to the actual performance of a windmill; however, differences between measured and computed performance can easily be explained within the framework of these aerodynamics uncertainties. The data used in this analysis come from reference 12, however, some cases are presented in which these data have been modified to simulate leading edge stall and surface roughness.

Comparison with Test Data

The results predicted by the analysis for a two blade configuration ($n = 2$) were compared with test data from references

3 and 4. The blade shape is a catenary with maximum radius of 2.13 m (7 ft) and a height of 4.27 m (14 ft). The shape of the upper half of a blade is represented by the curve shown on figure 5. The test Reynolds number was about 0.3×10^6 consequently low Reynolds number data were used for the NACA 0012 airfoil. The airfoil data were obtained from reference 12, and a tabulation of lift and drag coefficient and center of pressure versus angle of attack is presented in table 1. These data are for a Reynolds Number of 0.5×10^6 .

From the theoretical curve it is seen that the catenary VAW does not begin to produce sufficient power to overcome the drag due to stall until a velocity ratio of about 2.5 is reached. At this point the power coefficient increases with spin rate until a peak value of about .37 is reached. The power coefficient then decreases until at a velocity ratio of $R \approx 10$ it reaches zero. This determines the no load spin rate at which the windmill would operate.

The test data follows the same trends; however, there are differences between these results. The test data seemed to indicate that stall occurred at a higher velocity ratio and more abruptly than predicted, possibly indicating leading edge stall. Also, the no load velocity ratio reached in the tests was slightly greater than 8 indicating the zero lift drag was greater than predicted by smooth airfoil data. To demonstrate the effect of these variations on the predicted performance curve a computation was made using a zero lift drag coefficient representative of a rough surface.

Increasing C_{D_0} reduces the peak efficiency somewhat and causes the no load tip speed ratio to drop to a value of about 8.5. To demonstrate the effect of leading edge stall at low Reynolds number the lift and drag coefficient data were modified to reflect a sudden stall at an angle of attack of 10 degrees. These changes cause the peak value of power coefficient to be reduced slightly, and to occur at a higher tip speed ratio. Also, the no load point drops to about 8.6. For the catenary configuration the angle of attack variation along the blade is shown on figure 7 for $R = 4$ and $R = 5$, and at one angular location $\theta = 0$. As can be seen the angle of attack is almost constant over the majority of the blade and doesn't increase appreciable until the last 15 percent of the blade is reached. However, the contribution of this part of the blade to the total power production is small. Shown on figure 8 is the variation of peak angle of attack with R at the maximum radius. From this it can be seen that at values of $R \leq 4.5$ the peak angle of attack exceeds 10° consequently stall begins to set in. Since the angle of attack is essentially constant over the major part of the blade the whole blade stalls at about the same time thus causing the rapid reduction in the power coefficient curve as shown in figure 6.

If a system could be built with no losses other than aerodynamic its starting characteristics would consist of an initial rotation caused by the differential drag on the two blades. However, the angles of attack experienced would be higher than the stall angle and limiting spin rate would be reached where the moment generated by the lift force

would just balance that generated by the drag force. To get the windmill over this point some energy must be added to the system. Once the spin rate attains a value high enough such that the net torque due to lift is greater than that due to drag the system will spin up to the velocity ratio corresponding to no load condition.

The computed results for the case $n = 2$ are also shown plotted on figure 9 versus the induced velocity at the blades \tilde{V} . Included on this figure is a plot of the theoretical maximum curve obtained by setting the drag coefficient of the airfoil to zero.

As indicated previously no power is available until R reaches a value of about 2.5. As the spin rate increases the power curve follows the trend of the theoretical maximum curve although it is displaced somewhat. As the spin rate increases to values greater than about 6 the drag losses become more important since the angles of attack are decreasing and the contribution of the lift forces to the turning moment become of the same order as the retarding effects of the drag forces. Consequently the actual curve departs from the theoretical maximum by a large amount.

LINEAR THEORY FOR STRAIGHT BLADE CONFIGURATIONS

By restricting the possible windmill configurations to those with straight blades and by assuming that the blade aerodynamic coefficients vary linearly with angle of attack, closed form analytical expressions for windmill performance parameters are obtained. These expressions are used to study the effects on windmill performance of variations in aspect ratio and solidity.

Reduction to Analytical Form

Consider the special case of a straight blade configuration where $\bar{r} = 1.0$ and $\beta = 90^\circ$, both constant with respect to \bar{y} . From figure 3 we have

$$\bar{V}_r \sin \alpha = \bar{V} \cos \theta \quad (33a)$$

and

$$\bar{V}_r \cos \alpha = R - \bar{V} \sin \theta \quad (33b)$$

Also, if only small angles of attack are considered

$$C_L = K_1 \sin \alpha \quad (34a)$$

$$C_D \sim C_{D_0} \quad (34b)$$

With these approximations the thrust coefficient for one blade becomes

$$\begin{aligned} C_T(\theta) = \frac{\bar{c}}{2} \{ [K_1 \sin \alpha \cos \alpha \cos \theta + K_1 \sin^2 \alpha \sin \theta] \\ + C_{D_0} [\sin \alpha \cos \theta - \cos \alpha \sin \theta] \} \bar{V}_r^2 \end{aligned} \quad (35)$$

Substituting for \bar{V}_r yields

$$C_T(\theta) = \frac{\bar{c}}{2} \{ K_1 [\bar{V} (R - \bar{V} \sin \theta) \cos^2 \theta + \bar{V}^2 \cos^2 \theta \sin \theta] + \bar{V}_r C_{D_o} [\bar{V} - R \sin \theta] \} \quad (36)$$

and integrating over θ an average thrust coefficient C_{T_a} for n blades is obtained,

$$C_{T_a} = \frac{n\bar{c}}{4} K_1 \bar{V} R + \frac{n\bar{c}}{4\pi} \int_{\theta} [(R - \bar{V} \sin \theta)^2 + (\bar{V} \cos \theta)^2]^{\frac{1}{2}} (\bar{V} - R \sin \theta) C_{D_o} d\theta \quad (37)$$

Simplifying by assuming $(R - \bar{V} \sin \theta) \gg \bar{V} \cos \theta$ this becomes

$$C_{T_a} \sim \frac{n\bar{c} K_1 \bar{V} R}{4} + \frac{n\bar{c} C_{D_o}}{4\pi} \int_{\theta} (R - \bar{V} \sin \theta) (\bar{V} - R \sin \theta) d\theta$$

or

$$C_{T_a} = \frac{n\bar{c}}{4} R K_1 \bar{V} + 3 \frac{n\bar{c}}{4} \bar{V} R C_{D_o} \quad (38)$$

From momentum theory we have

$$C_{T_a} = 4 \bar{V} (1 - \bar{V})$$

therefore, equating these yields an expression for \bar{V} , the nondimensional velocity at the blade

$$\bar{V} = 1 - \frac{n\bar{c} R}{16} (K_1 + 3 C_{D_o}) \quad (39)$$

Using eq. (9) with $\bar{r} = 1$ and $\beta = 90^\circ$, the moment coefficient $C_M(\theta)$ can be written as

$$C_M(\theta) = \frac{2 \bar{Y}_m}{\bar{A}_s} \bar{c} \bar{V}_r^2 [(C_L \sin \alpha - C_D \cos \alpha) + \bar{c}(.5 - \bar{d}/\bar{c}) (C_L \cos \alpha + C_D \sin \alpha)] \quad (40)$$

but for a straight blade configuration $\bar{A}_s = 2 \bar{h}$

Using the relationships between \bar{V}_r & \bar{V} in equation (33)

yields

$$C_M(\theta) = \frac{\bar{c} K_1}{2} [\bar{V}^2 \cos^2 \theta + \bar{c} (.5 - \bar{d}/\bar{c}) \bar{V} \cos \theta (R - \bar{V} \sin \theta)] + \frac{\bar{c}}{2} (R - \bar{V} \sin \theta)^2 + \bar{V}^2 \cos^2 \theta [\bar{c} (.5 - \bar{d}/\bar{c}) C_{D_o} \bar{V} \cos \theta - C_{D_o} (R - \bar{V} \sin \theta)] \quad (41)$$

Restricting this analysis to cases in which $R - \bar{V} \sin \theta \gg \bar{V} \cos \theta$ equation 41 can be integrated over θ to yield the average moment

C_{M_a} as

$$C_{M_a} = \frac{n \bar{c} K_1}{4} \bar{V}^2 - \frac{n \bar{c} C_{D_o}}{4} (2R^2 + \bar{V}^2) \quad (42)$$

The power coefficient C_p is given by $C_p = R C_{M_a}$, substituting yields

$$C_p = R \frac{\bar{n}\bar{c} K_1}{4} \left(1 - \frac{\bar{n}\bar{c} R}{16} (K_1 + 3 C_{D_o})\right)^2 - \frac{\bar{n}\bar{c} C_{D_o}}{4} [2R^2 + \left(1 - \frac{\bar{n}\bar{c} R}{16} (K_1 + 3 C_{D_o})\right)^2] \quad (43)$$

where

$$K_1 = a_o \left[\frac{1 - a_o/\pi AR}{1 + a_o/\pi AR} \right]$$

Now for a straight blade

$$AR = \frac{h}{c} = \bar{h}/\bar{c} \quad (44)$$

therefore,

$$K_1 = a_o \left(\frac{1 - a_o \bar{c}/\pi \bar{h}}{1 - a_o \bar{c}/\pi \bar{h}} \right) \quad (45)$$

Equation (43) can be used to evaluate the effects of $\bar{n}\bar{c}$, \bar{h} , and C_{D_o} on performance of windmills. For the case where $C_{D_o} = 0$

the windmills performance reaches the theoretical maximum. This case along with a case using a representative value of C_{D_o} are

shown in figure 10. Both C_p and R are shown as a function of velocity ratio \bar{V} . Also shown on this figure are the results of the numerical analysis using nonlinear aerodynamics. As would be expected the linear and nonlinear results are in fairly good agreement at the higher spin rates; however, comparing these with the limiting value given by the $C_{D_o} = 0$ curve indicates that

significant improvements in performance could be realized if the airfoil drag could be reduced. For low spin rates the analytical and numerical results are in poor agreement due to the stall effects. The use of linear aerodynamics in the analytical solution causes the drag term to appear erroneously small so that the analytical results approach the theoretical maximum for low spin rates. This is due to the fact that the airfoil experiences high angles of attack and the contribution of the lift force is orders of magnitude greater than the retarding effect of the zero lift drag force.

Parameter Study

The analytical solutions can be used to evaluate the effects of solidity, and windmill aspect ratio on power coefficient. For small values of solidity, which is proportional to $\bar{n}\bar{c}$, and for high tip speed ratios these results are adequate to identify trends; however, at low tip speed ratios the effects of nonlinear airfoil characteristics become dominant and the analytical results are inaccurate. Figure 11 shows the analytical results as a function of solidity at a fixed aspect ratio. Power coefficient is plotted versus tip speed ratio and as indicated on the figure peak efficiency increases as solidity increases; however, the peak value occurs at a lower tip speed ratio and the range of tip speed ratios at which power can be supplied by the windmill varies inversely with solidity. Figure 12 shows the variation of power coefficient with \bar{h} as tip speed ratio varies. As can be seen \bar{h} does not have a major effect on windmill performance for the range

of values cited. In general as \bar{h} increases the aspect ratio of each blade increases consequently its performance improves. However, due to structural considerations it is desirable to design a windmill with as small a value of \bar{h} as possible without drastically and impairing performance.

When a numerical analysis based on the general theory is used to determine the effect of solidity on performance a major difference occurs for small values of tip speed ratio. These results are shown on figure 13. Since in this analysis the occurrence of airfoil stall is not dependent on solidity the minimum speed ratio at which power is produced is essentially the same for all configurations. Using the aerodynamic data for the NACA 0012 airfoil this value of tip speed ratio is about 2.5. The efficiency increases rapidly as tip speed ratio increases from this minimum value. However, for some values of solidity the peak efficiency would occur at tip speed ratios less than this minimum value were it not for stall effects. Consequently, with stall effects included, these peak values are never achieved. If a windmill could be designed using a blade which did not stall or stalled at a higher angle of attack it might be possible to achieved the higher performance indicated by the analytical solution. However, it remains questionable if one would want a design which responded so radically to changes in wind velocity.

CONFIGURATION EFFECTS ON AERODYNAMIC EFFICIENCY

Considering only aerodynamic efficiency the optimum VAW design as depicted in figure 14a would consist of straight blades attached to the center shaft by low drag struts. The windmill aspect ratio must be large enough to minimize losses due to blade aspect ratio. Unfortunately such a design leads to severe structural limitations due to the high bending loads which develop in the blade. It is for this reason that curved blades have been selected for designs currently in operation. With a curved blade the bending loads are greatly reduced and the centrifugal loads are reacted as almost pure tension loads in the blades. However, it is possible to design a straight bladed VAW which has the same structural capability as a curved blade VAW. This can be accomplished by supporting the blade at appropriate intervals as shown in figure 14c. Secondly, by placing the support struts at an angle other than 90 degrees from the axis of rotation they will produce enough lift force such that their lift induced torque is greater than the drag induced torque and they in effect contribute to the performance of the windmill.

The results of such a design are shown in figure 15 along with a comparison of the catenary VAW performance. For this configuration the support struts and the primary blade are an NACA 0012 airfoil. The strut to blade chord ratio is $1/2$. As the data indicates the peak power coefficient for the chevron design is about .43 compared to the value of .37 for the catenary. However, the catenary can produce power over a wider range of spin ratios than the chevron.

No attempt has been made to optimize the chevron design and one would expect that for higher values of h/r some improvement in performance could be expected. Also, the higher the angle of the support struts the greater will be their contribution. It is also possible to select a support strut angle such that the angle of attack at some point on the strut is the same as the angle of attack at the blade.

CONCLUSIONS

The results from the analysis presented herein indicate that a numerical solution using non-linear aerodynamic data and assuming a uniform induced velocity over the complete volume swept by the windmill can be used to predict performance of vertical axis windmills. The major parameters affecting windmill performance are the blade shape, blade aspect ratio and downwash effects. The effects of curved flow are insignificant providing the ratio of blade chord to diameter is small. The use of linear aerodynamics allows the defining torque equation to be integrated; however, these analytic solutions are incorrect at lower values of spin parameter where the aerodynamics are nonlinear. They are useful for assessing trends at higher spin parameter values. The performance of a VAW can be improved by using straight rather than curved blades provided the blade is supported in the proper manner. However, optimization of any VAW design will ultimately be based on the costs per installed unit of power consequently not only aerodynamic but also structural considerations must be taken into account.

PRECEDING PAGE BLANK NOT FILMED

REFERENCES

1. Wilson, Robert E.; and Lissaman, Peter B. S.: Applied Aerodynamics of Wind Power Machines. National Science Foundation, Oregon State University, May 1974.
2. South, P.; and Rangi, R. S.: Preliminary Tests of a High Speed Vertical Axis Windmill Model, National Research Council Canada, LTR-LA-74. March 1971.
3. South, P.; and Rangi, R. S.: A Wind Tunnel Investigation of 14 Ft. Diameter Vertical Axis Windmill, Canadian National Research Council, LTR-LA-105. September 1972.
4. Templin, R. J.: Aerodynamic Performance Theory for the NRC Vertical Axis Wind Turbine, National Research Council of Canada, LTR-LA-160. June 1974. .
5. Feltz, L. V.; and Blackwell, B. F.: An Investigation of Rotation Induced Stresses of Straight and of Curved Vertical Axis Wind Turbine Blades. Sandia Laboratories, March 1975.
6. Weingarten, L. I.; and Nickell, R. E.: Nonlinear Stress Analysis of Vertical Axis Wind Turbine Blades. Sandia Laboratories, April 1975.
7. Vadot, L.: A Synoptic Study of Different Types of Windmills, La Houille Blanche, No. 2, March/April 1957.
8. Donnasch, Daniel O.; Sherby, Sydney S.; and Cannolly, Thomas F.: Airplane Aerodynamics. Pitman Publishing Corporation, 1967.
9. Millikan, Clark B.: Aerodynamics of the Airplane. John Wiley and Sons, Inc., 1941.
10. Riegels, Friedrich W.: Aerofoil Sections, Butterworth and Co., LTD., 1961.
11. Gault, Donald E.: A Correlation of Low-Speed, Airfoil Section Stalling Characteristics with Reynolds Number and Airfoil Geometry, NACA TN-3963, March 1957.
12. Critzos, Chris C.; Heyson, Harry H.; and Boswinkle, Robert W., Jr.: NACA 0012 Report - Aerodynamic Characteristics of the NACA 0012 Airfoil Section at Angles of Attack from 0° to 180° , NACA Technical Note 3361.

APPENDIX

WINDMILL PERFORMANCE PREDICTION COMPUTER PROGRAM

Order of Input

1. Header Card, Columns 1 through 80.
2. Namelist \$NAM1 including:

<u>Fortran Symbol</u>	<u>Engineering Symbol</u>	<u>Definition</u>
AR	AR	Aspect ratio of blade
ARS	AR_s	Aspect ratio of lifting struts
AZ	a_z	Section lift curve slope
BETA(I)	β	Array of local slope of blade for each YBAR(I)
BETS	β_s	Angle of lifting struts
CBAR	\bar{c}	Nondimensional blade chord
CBARS	\bar{c}_s	Chord of lifting and nonlifting struts
CD(I)	C_D	Array of Section drag coefficient of blade and struts for each GAM(I)
CD1	C_{D1}	Zero lift drag coefficient of nonlifting struts
CK1	CK1	Number of nonlifting struts
CL(I)	C_L	Array of Section lift coefficient of blade and struts for each GAM(I)
CMC4(I)	$C_{M_{c/4}}$	Quarter chord pitching moment coefficient
DY	DY	Increment used to calculate y coordinate array for blade, from YMIN to YMAX.
DYS	DY_s	Increment used to calculate Y coordinate array for struts from YSMIN to YSMAX.
GAM(I)	γ	Array of angle of attack, where I = 1, NGAM.

APPENDIX - CONTINUED

<u>Fortran Symbol</u>	<u>Engineering Symbol</u>	<u>Definition</u>
ITHPRNT		Total number of THPRNT values, maximum is 10.
N	n	Number of blades
NGAM		Total number of GAM values, maximum is 100.
NS	n_s	Number of lifting struts, if none set = 0.
NTHETA		Total number in THETA array, maximum is 200.
NVR		Total number in VRRY array, maximum is 10.
NY		Total number in YBAR array, maximum is 50.
RBAR(I)	\bar{r}	Array of windmill blade radius for each YBAR(I).
TC	τ	Blade airfoil thickness ratio.
THETA(I)	θ	Array of windmill angular coordinate, degrees, where I = 1, NTHETA.
THPRNT(I)		Array of THETA values at which the lift, drag and moment values can be printed, where I = 1, ITHPRNT.
VRRY(I)	R	Array of specified velocity ratios at which the windmill is to be analyzed, where I = 1, NVR.
YBAR(I)	\bar{y}	Array of coordinates along the axis of rotation of the windmill, where I = 1, NY.
YMAX	\bar{Y}_{\max}	Maximum Y coordinate of blade.
YMIN	\bar{Y}_{\min}	Minimum Y coordinate of blade.
YSMAX	\bar{Y}_{smax}	Maximum y coordinate of lifting struts
YSMIN	\bar{Y}_{smin}	Minimum y coordinate of lifting struts

APPENDIX - CONTINUED

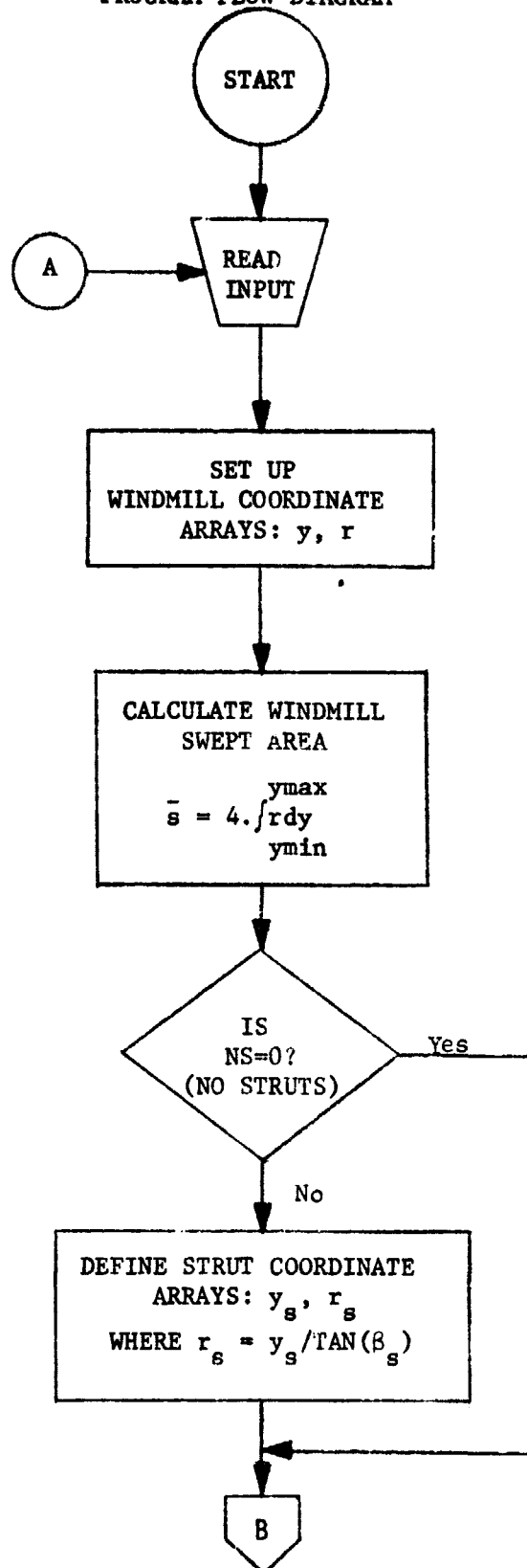
Output Parameters

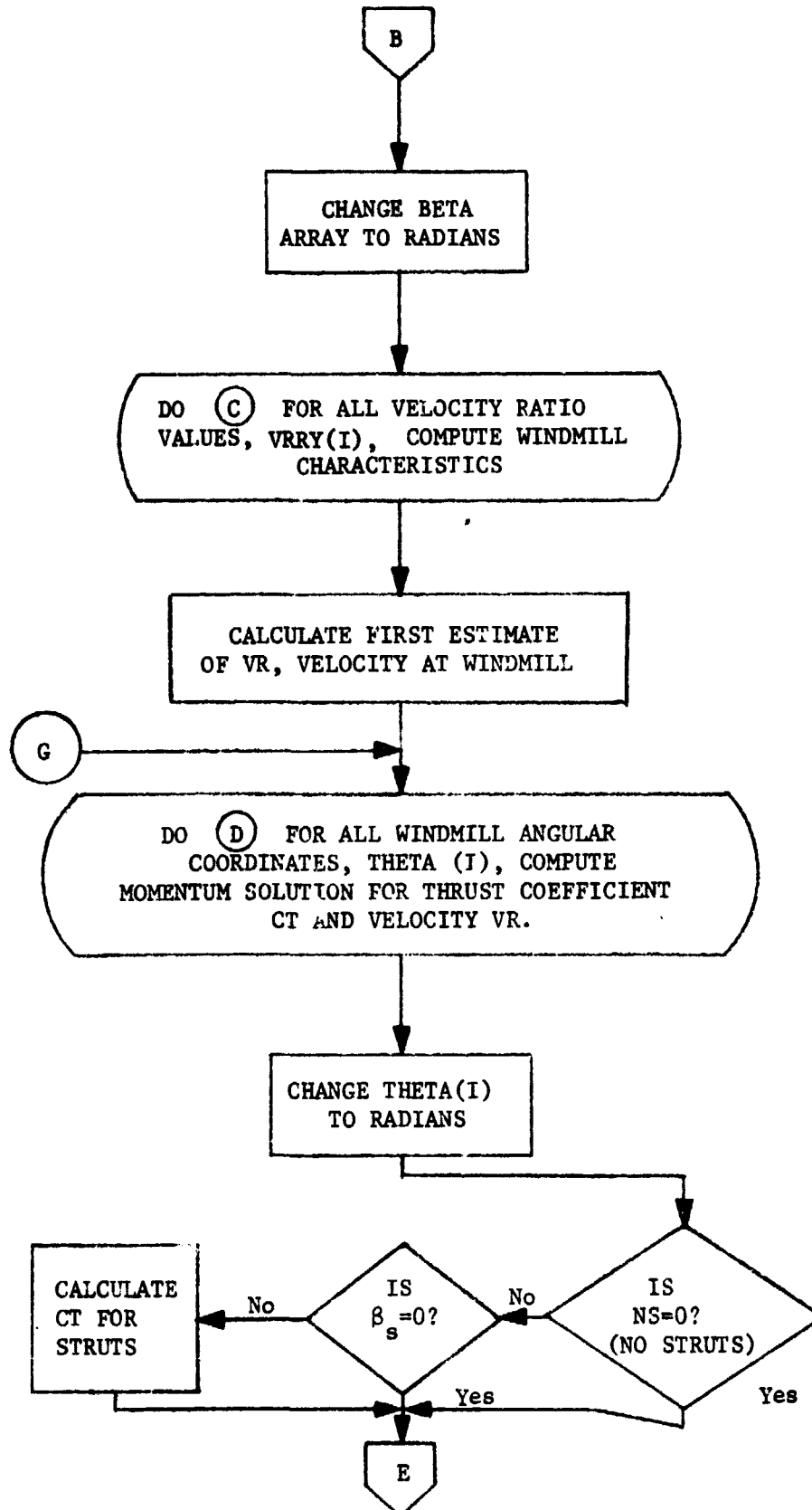
<u>Output Symbol</u>	<u>Engineering Symbol</u>	<u>Definition</u>
BARCT	C_{T_a}	Windmill thrust coefficient averaged over a revolution
CD	C_D	Airfoil section drag coefficient
CL	C_L	Airfoil section lift coefficient
CM(THETA)	$C_M(\theta)$	Blade moment coefficient for angular location θ
CMA	C_{M_a}	Average windmill moment coefficient
CMAS	$C_{M_{as}}$	Average moment coefficient due to struts
CMC4	$C_{M_{c/4}}$	Airfoil section quarter chord moment coefficient
CMS(THETA)	$C_{M_s}(\theta)$	Strut moment coefficient for angular location θ
CMT	$C_{M_T}(\theta)$	Total moment coefficient for n blades at angular location θ
CMTS	$C_{M_{TS}}(\theta)$	Total moment coefficient for all struts at angular location θ
CPA	C_{P_a}	Power coefficient due to lifting blades and struts
CPL	C_{P_l}	Power coefficient loss due to nonlifting struts
CPN	C_{P_n}	Net power coefficient
D/C	d/c	Location of center of pressure measured chordwise from the airfoil leading edge in fractions of the chord length

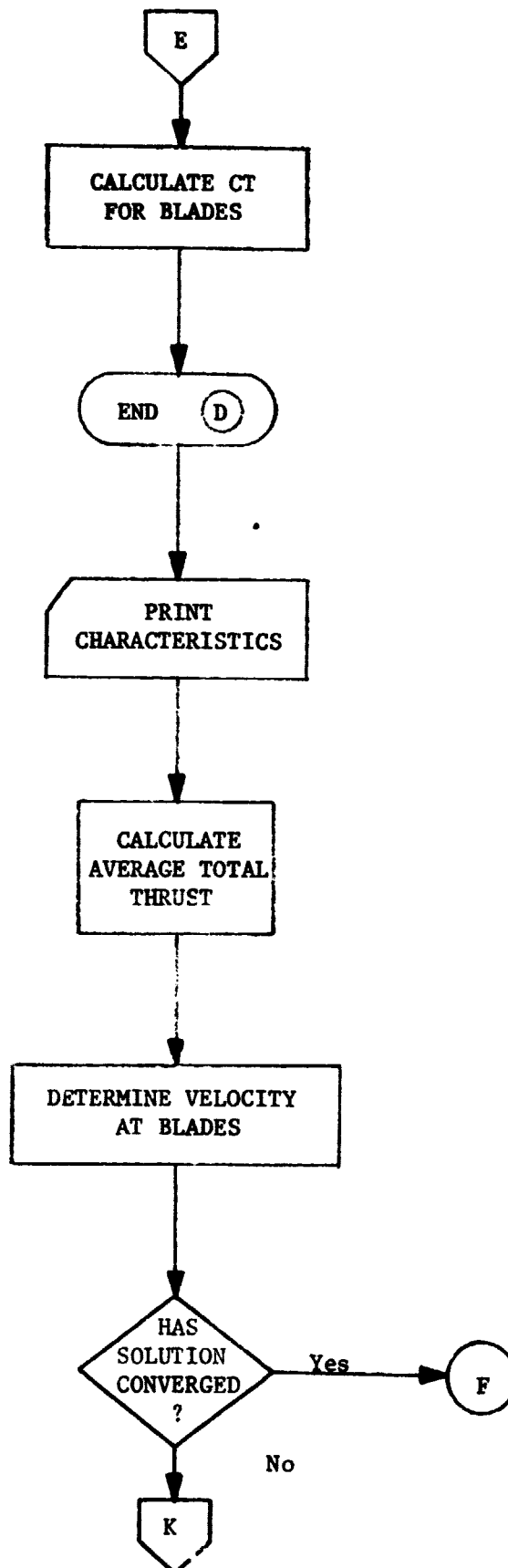
APPENDIX - CONTINUED

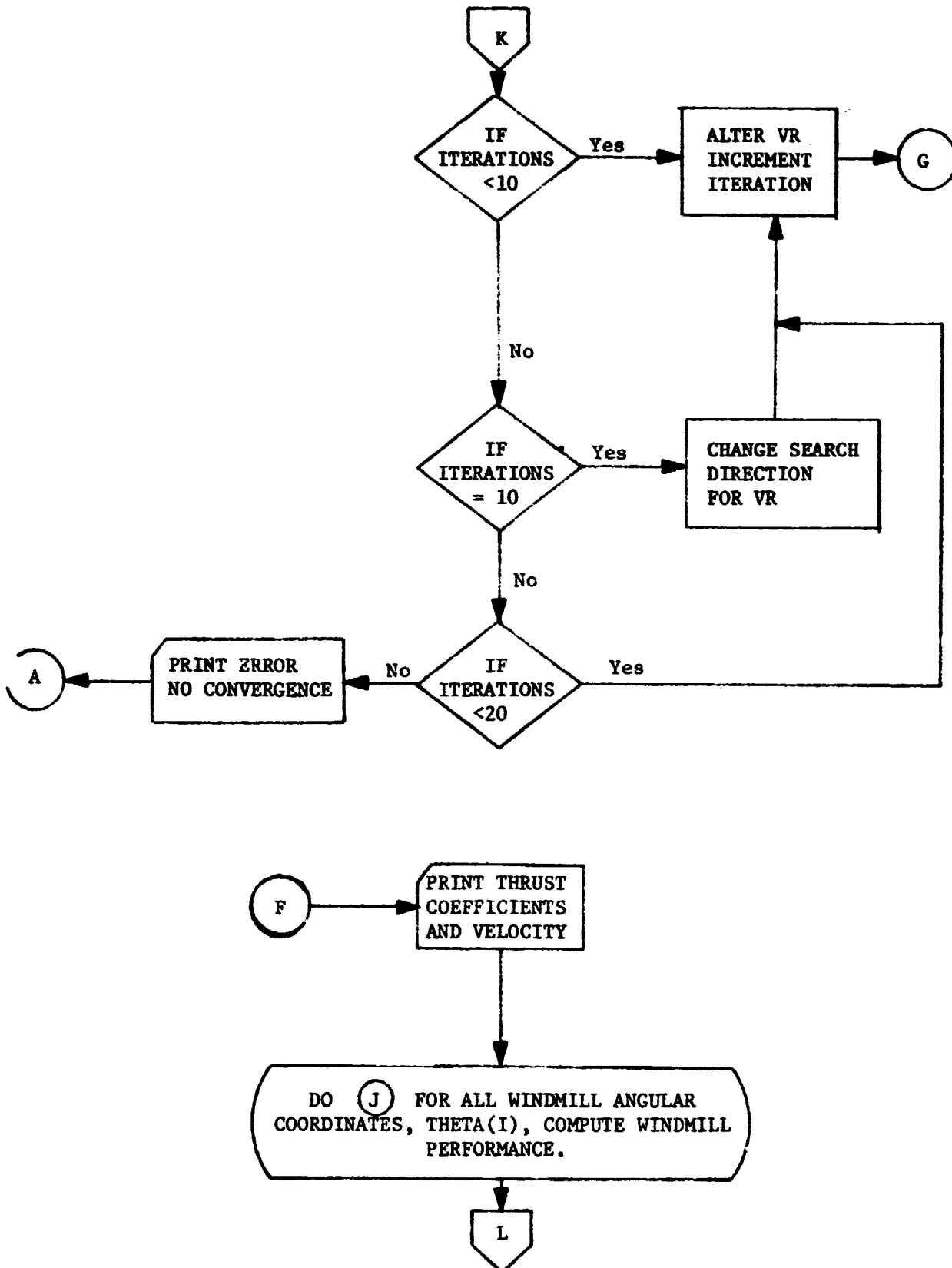
<u>Output Symbol</u>	<u>Engineering Symbol</u>	<u>Definition</u>
DEL CM	ΔC_M	Incremental moment coefficient due to a blade element
GAMMA	γ	Local blade angle of attack
OMEGA	ω	Windmill rotational speed
RMAX	r_{\max}	Maximum windmill radius
SBAR	\bar{S}	Nondimensional windmill projected area in a vertical plane
THETA	θ	Angle of windmill rotation measured from the free wind direction
VINF	V_{∞}	Wind stream speed at a large distance from the windmill
VR	V	Wind stream speed at the windmill

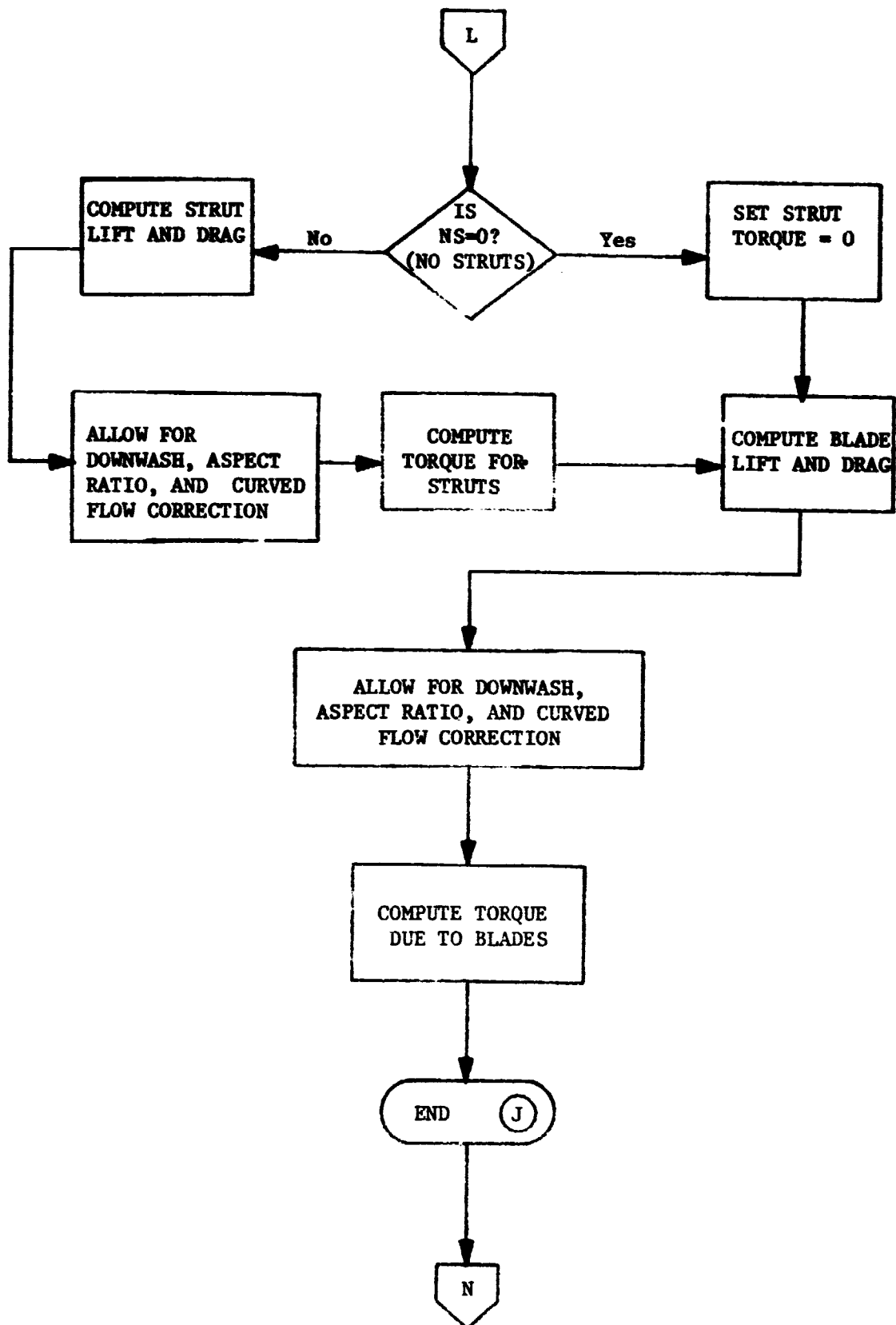
APPENDIX - CONTINUED
PROGRAM FLOW DIAGRAM

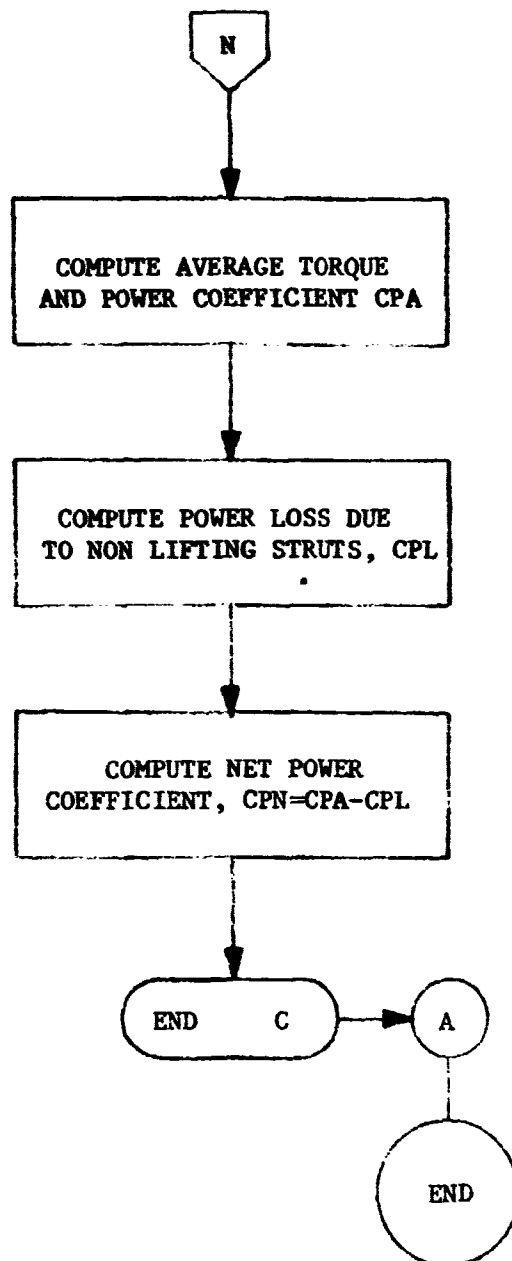












PROGRAM A4425(LVPM,OUTLINE,LEVELN2J,IAPE5=DJIPU1)

C TITLE - WINDMILL EFFICIENCY ANALYSIS

C ENGINEERS- RA PH MORAGA AND RAY DABENHART

C PROGRAMMER - MARIA SIOPHENS

C EXTERNALS- CLCLO

C DIMENSION HETA(50), VDI(100), CL(100), CM(100), CMC4(100), CI(200),

VCIS(200), GAA(100), WEDE 2(6), MC(100), PSI(50), RMAR(50),

2RRETA(50), 2R(200), 2S(100), SJM(200), SUNCN(200), SU4CMS(200),

JSUMCIS(200), SU4S(200), THETA(200), T-PRNT(10), V2HAR(50),

AV2RA(200), V2RY(20), YHAR(50), YR(200), YS(100)

C COMMON/AMSUB/CAPR

C NAMELIST/NAME/AR,AMS,AZ,BETA,BEIS,CHARS,CD,CDI,CL,CL,CMC4,

IDY,DYS,GAM, ITHPRNT,N,NDAM,NS,NHETA,NVR,NY,RRAM,IC,THETA,

2I-PRNT,V2RY,YHAR,Y2RA,YMIN,YMAX,YSMIN

C ORDER OF I N P U T

C 1. HEADER CARD

C 2. NAMELIST NAME INCLUDING-

C AR - ASPECT RATIO OF BLADE

C AMS - ASPECT RATIO OF LIFTING SURFIS

C AZ - SECTION LIFT CURVE SLOPE

C BETA - LOCAL SLOPE OF BLADE FOR EACH YEAR

C BEIS - ANG. E OF LIFTING SURFIS

C CHAZ - NONDIMENSIONAL BLADE CHORD

C CHARS - CHORD OF LIFTING AND NONLIFTING SURFIS

C CD - SECTION DRAG COEFFICIENT OF BLADE AND SURFIS FOR EACH GAM

C CDI - ZERO LIFT OF S COEFFICIENT OF NONLIFTING SURFIS

C CKI - NUMBER OF NONLIFTING SURFIS

C CL - SECTION LIFT COEFFICIENT OF BLADE AND SURFIS FOR EACH GAM

C CMC4 - QUARTER CHORD MOMENT COEFFICIENT

C DY - INTEGRANT USED TO CALCULATE Y COORDINATE ARRAY FOR BLADE

C E202 Y2A10 Y2A4

C DYS - INTEGRANT USED TO CALCULATE Y COORDINATE ARRAY FOR SURFIS

C E202 Y2A10 Y2A4A

C GAM - ANG. E OF ATTACK ARRAY

C ITHPRNT - ITHPR, NUMBER OF ITHPR VALUES, MAXIMUM IS 10.

APPENDIX - CONTINUED

COMPUTER PROGRAM LISTING

ORIGINAL PAGE IS
OF POOR QUALITY

APPENDIX - CONTINUED

```

C N - NUMBER OF BLADES
C NGAM - TOTAL NUMBER OF GAM VALUES, MAXIMUM IS 100
C NS - NUMBER OF LIFTING STRUTS, IF NONE SET =0
C NTHETA - TOTAL NUMBER IN THETA ARRAY, MAXIMUM IS 200
C NVR - TOTAL NUMBER IN VARY ARRAY, MAXIMUM IS 10
C NY - TOTAL NUMBER IN YBAR ARRAY, MAXIMUM IS 50
C RBAR - WINDMILL BLADE RADIUS FOR EACH YEAR
C TC - BLADE AIRFOIL THICKNESS RATIO
C THETA - ARRAY OF WINDMILL ANGULAR COORDINATES, DEGREES,
C THPRNT - ARRAY OF THETA VALUES AT WHICH THE LIFT, DRAG, AND MCMENT
C - VALUES CAN BE PRINTED
C VRRY - ARRAY OF SPECIFIED VELOCITY RATIOS AT WHICH THE WINDMILL IS TO BE
C - ANALYSED
C YBAR - ARRAY OF COORDINATES ALONG THE AXIS OF ROTATION OF THE WINDMILL
C YMAX - MAXIMUM Y COORDINATE OF BLADE
C YMIN - MINIMUM Y COORDINATE OF BLADE
C YSMAX - MAXIMUM Y COORDINATE OF LIFTING STRUTS
C YSMIN - MINIMUM Y COORDINATE OF LIFTING STRUTS
C
C
C CBARS=0.
C RADANS=.0174532925
C
C READ HEADER CARD AND INPUT DATA
C
000006 1 READ(5,104,HEADER
000014 IF(EDF,5)2,3
000017 2 STOP
000021 3 READ(5,NAM1)
000024 DO 5 I=1,NGAM
000026 G = GAM(I)*RADANS
000030 CN = CL(I)*CCS(G)+CD(I)*SIN(G)
000040 DELTA = 0.01*ABS(CN)
000042 IF (-DELTA.LE.CN.AND.CN.LE.DELTA) GO TO 7
000054 GO TO 5
000054 7 HC(I) = 0.25
000056 GO TO 5
000057 6 HC(I) = 0.25 - CMC4(I)/CN
000063 5 CONTINUE
000066 WRITE(6,105)HEADER
000073 WRITE(6,NAM1)
000076 WRITE(6,115)(GAM(I),CL(I),CD(I),CMC4(I),HC(I),I=1,NGAM)
C

```


C SET UP WINDMILL COORDINATES RR VS. YR

C

```

000121 I=0
000122 YR(1)=YMIN
000124 10 I=I+1
000126 CALL FTLUP(YR(I),RR(I),I,NY,YBAR,RBAR)
000132 YR(I+1)=YR(I)+DY
000135 IF(YR(I+1).LT.YMAX)GO TO 10
000140 I=I+1
000141 YR(I)=YMAX
000142 RR(I)=RBAR(NY)
000145 IT=1

```

C CALCULATE SBAR - WINDMILL SWEEP AREA

C

```

000146 CALL TRAP(RR,YR,IT,SUM,0.)
000151 SBAR=4.*SUM(IT)
000154 WRITE(6,106)SBAR
000161 BARCTS=0.

```

C

C SET UP STRUT COORDINATES RS VS. YS

C

```

000162 NS=0, NO STRUTS
000163 IF(NS.EQ.0)GO TO 19
000165 BETSR=BETS*RADIANS
000167 TB=TAN(BETSR)
000171 YS(1)=YSMIN
000171 K=1

```

15 RS(K)=YS(K)/TB

K=K+1

YS(K)=YS(K-1)+DYS

IF(YS(K).LT.YSMAX)GO TO 15

YS(K)=YSMAX

RS(K)=YS(K)/TB

KS=K

19 CONTINUE

DO 20 I=1,NY

RBETA(I)=RADIANS*BETA(I)

20 CONTINUE

C

C BEGIN COMPUTATION OF WINDMILL CHARACTERISTICS FOR EACH VELOCITY RATIO-VR

C

```

000215 DO 70 IVR=1,NVR
000217 CAPR=VPRY(IVR)

```

APPENDIX - CONTINUED

ORIGINAL PAGE IS
OF POOR QUALITY

```

000221      WRITE(6,109)CAPR
000226      VVR=1./CAPR
000230      ITER=1

```

```

C
C FIRST ESTIMATE OF VR, VELOCITY AT THE WINDMILL
C

```

```

000231      VR = 1. - N*CBAR*3.14159*CAPR/8.
000237      25 CONTINUE

```

```

C
C CALCULATE MOMENTUM SOLUTION FOR THRUST COEFFICIENT CT AND VELOCITY VR
C

```

```

000237      DO 40 I=1,NTHETA
000241      TH=THETA(I)*RADIANS
000243      IF(NS.EQ.0)GO TC 35
000244      IF(BETS.EQ.0.)GO TO 35

```

```

C
C CALCULATE CT FOR STRUTS
C

```

```

000245      DO 30 K=1,KS
000247      CALL GAMMA(AGAMS,SGAMS,CGAMS,VBAR2S,TH,DETSR,VR,RS(K))
000261      GAMM=ABS(AGAMS)/RADIANS
000264      CALL FTLUP(GAMM,TCL,I,NGAM,GAM,CL)
000270      CALL FTLUP(GAMM,TCD,I,NGAM,GAM,CD)
000274      CALL FTLUP(GAMM,THC,I,NGAM,GAM,HC)
000300      IF(AGAMS.LT.0.)TCL=-TCL
000303      TCL=TCL/(1.+AZ/(3.14159*ARS))*(1.-AZ/(3.14159*ARS))

```

```

C CURVED FLOW CORRECTION

```

```

000313      TCL=TCL*CLCLO(CAPR,CBAR,TH)
000317      TCD=TCD+TCL*2/(3.14159*ARS)
000323      CT(K)=VBAR2S*((TCL*SGAMS-TCD*CGAMS)*SIN(TH)+(TCL*CGAMS+TCD*SGAMS))*

```

```

1SIN(BETSR)*COS(TH))/SIN(BETSR)

```

```

30 CONTINUE

```

```

000351      CALL TRAP(CT,YS,KS,SUM,0.)
000353      SUMCTS(I)=SUM(KS)*2.*NS*CBARS/SEAR
000357
000365      35 CONTINUE

```

```

C
C CALCULATE CT FOR BLADES
C

```

```

000365      DO 39 J=1,IT
000367      CALL FTLUP(YR(J),BET,I,NY,YBAR,RBETA)
000373      CALL GAMMA(AGAM,SGAM,CGAM,VBAR2, TH,BET,VR,RR(J))
000405      GAMM=ABS(AGAM)/RADIANS
000410      CALL FTLUP(GAMM, TCL,I,NGAM,GAM,CL)

```

APPENDIX - CONTINUED

APPENDIX - CONTINUED

ORIGINAL PAGE IS
OF POOR QUALITY

```

000414 CALL FTLUP(GAMM, TCD,1,NGAM,GAM,CD)
000420 CALL FTLUP(GAMM, THC,1,NGAM,GAM,HC)
000424 IF(AGAM.LT.0.)TCL=TCL
000427 TCL=TCL/(1.+AZ/(3.14159*AR))*((1.-AZ/(3.14159*AR)))
C CURVED FLOW CORRECTION
000437 TCL=TCL*CLCLO(CAPR,CBAR,TH)
000443 TCD=TCD+TCL**2/(3.14159*AR)
000447 CT(J)=VBAR2*((TCL*SGAM-TCD*CGAM)*SIN(TH)+(TCL*CGAM+TCD*SGAM)*
1SIN(BET))*COS(TH))/SIN(BET)
000475 39 CONTINUE
000477 CALL TRAP(CT,YR,IT,SUM,0.)
000503 SUMCM(I)=SUM(IT)*2.*N*CBAR/SBAR
000511 40 CONTINUE
C
C CALCULATE AVERAGE TOTAL THRUST
C
000514 CALL TRAP(SUMCM,THETA,NTHETA,SUM,0.)
000517 BARCT=1./360.*SUM(NTHETA)
000522 IF(NS.EQ.0)GO TO 44
000523 IF(BETS.EQ.0)GO TO 42
000524 CALL TRAP(SUMCTS,THETA,NTHETA,SUM,0.)
000530 CTSSUM=SUM(NTHETA)
000532 BARCTS=1./360.*CTSSUM
000535 WRITE(6,114)SUMCTS(NTHETA)
000542 GO TO 44
000543 42 BARCTS=NS*CD(1)*CBARS*VR/(2.*SBAR)
000551 44 BARTT=BARCT+BARCTS
C
C DETERM VELOCITY AT BLADES
C
000553 FV=VR**2- VR*BARTT/4.
C
C CHECK ON CONVERGENCE OF SOLUTION
C
000557 IF(ITER.NE.1)GO TO 46
000561 C=.1
000562 SAVVR=VR
000564 SAVFV=FV
000566 GO TO 48
000566 46 IF(STF*FV.LT.0.)GO TO 49
000571 IF(ITER.LT.10)GO TO 48
000573 IF(ITER.EQ.10)GO TO 150
000574 IF(ITER.GT.10.AND.ITER.LT.20)48,70

```

APPENDIX - CONTINUED

```

000604 150 VR=SAVVR
000605 FV=SAV FV
000607 C=-.1
000611 48 STF=FV
000612 STV=VR
000614 VR=VR+C*VR
000616 ITER=ITER+1
000620 GO TO 25

```

C SOLUTION HAS CONVERGED, CT AND VR

```

000620 49 XV=-STF*(VR-STV)/(FV-STF)+STV
000626 VR=XV
000630 WRITE(6,113)BARCT,VR,ITER
000642 IF=1
000643 IF(ITHPRNT.EQ.0)IF=0

```

C CALCULATE THE PERFORMANCE FOR A GIVEN VARY, FOR ALL THETAS

```

000645 DO 90 I=1,NTHETA
000647 NPRNT=0
000650 IF(IF.EQ.0)GO TO 54
000651 IF(THETA(I).EQ.ITHPRNT(IF))53,54
000656 53 WRITE(6,100)THETA(I)
000664 NPRNT=1
000665 IF=IF+1
000667 IF(IF.GT.ITHPRNT)IF=0
000672 54 CONTINUE
000672 TH=THETA(I)*RADIAN
000674 IF(NS.EQ.0)GO TO 51
000676 IF(BETS.NE.0)GO TO 52
000677 51 SUMCMS(I)=0.
000701 GO TO 58

```

C COMPUTE STRUT LIFT AND DRAG

```

000701 52 CONTINUE
000701 IF(NPRNT.EQ.1)WRITE(6,116)
000707 DO 56 K=1,KS
000711 CALL GAMMA(AGAMS,EQ2,EQ1,EQ,TH,BETSR,VR,RS(K))
000723 GAMDEG=AGAMS/RADIANS
000725 GAMM=ABS(AGAMS)/RADIANS

```

APPENDIX - CONTINUED

ORIGINAL PAGE IS
OF POOR QUALITY

```

000727      CALL FTLUP(GAMM , TCL,1,NGAM,GAM,CL)
000733      CALL FTLUP(GAMM , TCD,1,NGAM,GAM,CD)
000737      CALL FTLUP(GAMM , THC,1,NGAM,GAM,HC)
000743      IF(AGAMS.LT.O.)TCL=-TCL
C
C      DOWNWASH AND ASPECT RATIO CORRECTION
C
000746      TCL=TCL/(1.+AZ/(3.14159*ARS))*(1.-AZ/(3.14159*ARS))
C      CURVED FLOW CORRECTION
000757      TCL=TCL*CLCLO(CAPR,CBAR,TH)
000763      TCD=TCD+TCL*2/(3.14159*ARS)
000767      IF(RS(K).EQ.O.)GO TO 55
C
C      TORQUE DUE TO STRUTS
C
000771      CM(K)=2.*CBARS*RS(K)/SBAR*EQ* (CBARS/RS(K)*(.5-THC)*(EQ1*TCL+EQ2*
ITCD)+1./SIN(BETSR)*(EQ2*TCL-EQ1*TCD))
GO TO 57
001020      55 CM(K)=0.
001020      57 IF(INPRNT.EQ.1)WRITE(6,101)YS(K),GAMDEG,TCL,TCD,THC,CM(K)
001022      56 CONTINUE
001044      CALL TRAP(CM,YS,KS,SUM,O.)
001047      SUMCMS(1)=SUM(KS)
001052      58 CONTINUE
001055      IF(INPRNT.EQ.1)WRITE(6,117)
001055      DO 50 J=1,IT
001053
C
C      COMPUTE BLADE LIFT AND DRAG
C
001065      CALL FTLUP(YR(J),BET,1,NY,YBAR,RBETA)
001071      CALL GAMMA(AGAM,EQ2,EQ1,EQ,TH,BET,VR,RR(J))
001103      GAMDEG=AGAM/RADIANS
001105      GAMM =ABS(AGAM)/RADIANS
001107      CALL FTLUP(GAMM , TCL,1,NGAM,GAM,CL)
001113      CALL FTLUP(GAMM , TCD,1,NGAM,GAM,CD)
001117      CALL FTLUP(GAMM , THC,1,NGAM,GAM,HC)
001123      IF(AGAM.LT.O.)TCL=-TCL
C
C      DOWNWASH AND ASPECT RATIO CORRECTION
C
001126      TCL=TCL/(1.+AZ/(3.14159*AR))*(1.-AZ/(3.14159*AR))
C      CURVED FLOW CORRECTION
001137      TCL=TCL*CLCLO(CAPR,CBAR,TH)

```

APPENDIX - CONTINUED

001143 TCD=TCD+TCL*#2/(3.14159*AR)

C

C TORQUE DUE TO BLADE

C

001147 CM(J)=2.*CBAR*RR(J)/SBAR*EQ* (CBAR/RR(J))*(.5-THC)*(EQ1

1*TCL+EQ2*TCD)+1./SIN(BET)*(EQ2*TCL-EQ1*TCD))

IF(NPRNT.EQ.1)WRITE(6,101)YR(J),GAMDEG,TCL,TCD,THC,CM(J)

001176 50 CONTINUE

001217 CALL TRAP(CM,YR,IT,SUM,O.)

001222 SUMCM(I)=SUM(IT)

001225 IF(NPRNT.EQ.1)WRITE(6,102)THETA(I),SUMCM(I)

001230 90 CONTINUE

001241 WRITE(6,103)(THETA(I),SUMCM(I),SUMCMS(I),I=1,NTHETA)

C

C COMPUTE TOTAL AVERAGE TORQUE AND POWER COEFFICIENT CPA

C

001262 NN=NTHETA/N

001265 DO 80 I=1,NN

001267 CTS(I)=0.

001270 80 CT(I)=0.

001274 DO 60 J=1,N

001275 NJ=(J-1)*NN

001300 DO 60 I=1,NN

001302 CT(I)=CT(I)+SUMCM(I+NJ)

001306 CTS(I)=CTS(I)+NS*SUMCMS(I+NJ)

001312 60 CONTINUE

001317 CALL TRAP(CT,THETA,NN,SUM,O.)

001323 CALL TRAP(CTS,THETA,NN,SUMS,O.)

001327 DO 65 I=1,NN

001331 SUM(I)=N*SUM(I)/360.

001334 SUMS(I)=N*SUMS(I)/360.

001337 65 CONTINUE

001341 WRITE(6,108)N,(THETA(I),CT(I),CTS(I),I=1,NN)

001361 WRITE(6,111)SUM(NN),SUMS(NN)

001371 CPA=(SUM(NN)+SUMS(NN))/VVR

C

C COMPUTE POWER LOSS DUE TO NONLIFTING STRUTS,CPL

C

001374 CPL=(CK1*CBARS*CD1)*(1.+(VR/CAPR)**2)/(4.*SBAR*VVR**3)

001405 CPN=CPA-CPL

001407 WRITE(6,110)CPA,CPL,CPN

001421 70 CONTINUE

001424 GO TO 1

C
C F O R M A T S
C

```

001424 100 FORMAT(/5X,*THETA =,F12.2)
001424 101 FORMAT(E15.7,F10.2,5E15.7)
001424 102 FORMAT(/1X*CM(,F5.1*)=,E15.7)
001424 103 FORMAT(1H1,10X*MOMENT COEFFICIENT FOR ONE BLADE AND SUPPORTING STRUTS*/5X*THETA*5X*CM(THETA)*6X*CMS(THETA)*/(F10.2,2E16.7))
001424 104 FORMAT(8A10)
001424 105 FORMAT(1H1,10X*PROGRAM A4426 - WINDMILL EFFICIENCY ANALYSIS*/11X 18A10)
001424 106 FORMAT(1H1,20X*OUTPUT*//* NONDIMENSIONAL WINDMILL SWEEP AREA SBAR=1*E15.7)
001424 107 FORMAT(//* CP =,E15.7)
001424 108 FORMAT(1H1,5X*NUMBER OF BLADES =,I3/5X*THETA*8X*CMT*12X*CMTS*1/(F10.2,2E15.7))
001424 109 FORMAT(1H1,33H VELOCITY RATIO RMAX*OMEGA/VINF =,F12.4//)
001424 110 FORMAT(//* POWER COEFFICIENT WITHOUT NONLIFTING STRUT LOSSES,CPA=,1E15.7/* POWER LOST DUE TO NONLIFTING STRUTS, CPL=,E15.7/2* NET POWER COEFFICIENT, CPN=,E15.7)
001424 111 FORMAT(//* AVERAGE BLADE MOMENT COEFFICIENT, CMA =,E15.7/* AVERAGE STRUT MOMENT COEFFICIENT, CMAS =,E15.7)
001424 113 FORMAT(//* WINDMILL THRUST COEFFICIENT BARCT =,E15.7/* VR =,E15.7/1* ITERATIONS =,I5)
001424 114 FORMAT(* CTS =,E15.7)
001424 115 FORMAT(1H1,20X*INPUT TABLES*/6X*GAMMA*7X*CL*14X*CD*13X*CMC4*13X*DI/C*/(F12.4,4E15.7))
001424 116 FORMAT(/5X*WINDMILL STRUT LIFT, DRAG AND MOMENT*/6X*YSBAR*,8X1*GAMMA*10X*CL*13X*CD*12X*D/C*10X*DEL CMS*)
001424 117 FORMAT(/,5X*WINDMILL BLADE LIFT, DRAG AND MOMENT*/7X*YBAR*8X*GAMMA1*10X*CL*13X*CD*12X*D/C*10X,*DEL CM*)
001424 END

```

APPENDIX - CONTINUED

ORIGINAL PAGE IS
OF POOR QUALITY

APPENDIX - CONTINUED

```

000010 SUBROUTINE TRAP(Y,X,NL,SUM,SUM1)
000010 DIMENSION Y(NL),X(NL),SUM(NL)
000010 SUM(1)=SUM1
000011 NLM=NL-1
000012 DO 1 N=1,NLM
000014 NP=N+1
000015 1 SUM(NP)=SUM(N):(Y(NP)+Y(N))*(X(NP)-X(N))/2.
000034 RETURN
000035 END

```


C SUBROUTINE GAMMA(GAM, SCAM, CGAM, VBAR2, TH, BET, VR, RR)
 C
 C CALCULATE THE LOCAL ANGLE OF ATTACK GAMMA(I.E. ALPHA), AND THE
 C LOCAL VELOCITY VBAR
 C

000013 CCOMMON/GAMSUB/CAPR

000013 C
 000013 PART1=RR*CAPR-VR*SIN(TH)
 000024 PART2=VR*COS(TH)*SIN(BET)
 000042 GAM=ATAN2(PART2,PART1)
 000051 DENC=SQRT(PART1**2+PART2**2)
 000055 SGAM=PART2/DENO
 000062 CGAM=PART1/DENO
 000064 VBAR2=PART1**2+(VR*COS(TH))**2
 000074 RETURN
 000075 END

APPENDIX - CONTINUED

ORIGINAL PAGE IS
OF POOR QUALITY

APPENDIX - CONTINUED

FUNCTION CLCLO(CAPR,CBAR,TH)
 FUNCTION CLCLO CORRECTS LIFT COEFFICIENT FOR FLOW CURVATURE EFFECTS

C

000006
 000006
 000011
 000015
 000017
 000026
 000037
 000050
 000063
 000075
 000077
 000077

REAL NUM
 COSH=COS(TH)
 SINH=SIN(TH)
 A=CAPR*CBAR/2.
 ALPHAO=ATAN2(COSH,CAPR-SINH)
 ALPHA1=ATAN2(COSH-A,CAPR-SINH)
 ALPHA2=ATAN2(COSH+A,CAPR-SINH)
 NUM=(CAPR-SINH)*(COS(ALPHA1)-COS(ALPHA2))/CAPR.
 DENOM=(COS(ALPHAO))*2*SIN(ALPHAO)*CBAR
 CLCLO=NUM/DENOM
 RETURN
 END

```

SUBROUTINE FTLUP(X,Y,M,N,VARI,VARD)
  DIMENSION VARI(1),VARD(1),V(3),YY(2)
  IF (M.EQ.O.AND.M.EQ.O) GO TO 1
  IF (M.EQ.O.AND.N.NE.O) GO TO 97
  IF (N.LE.IABS(M), GO TO 97
  IF (M.GT.O) GO TO 31
  M.LT.O
  DO 44 IYY=1,N
  I=IYY
  IF (VARI(I)-X)800,119,44
  44 CONTINUE
  I=N+M
  C
  IF X.LT.X(N),EXTRAPCLATE
  IF (M.EQ.-1)GO TO 801
  GO TO 802
  IF X.GT.X(1),EXTRAPCLATE
  800 IF (I.EQ.1.AND.M.EQ.-1)GO TO 801
  IF (I.EQ.1.AND.M.EQ.-2)GO TO 802
  IF (M.NE.-1)GO TO 622
  M=-1
  C
  I=1-1
  801 IF (VARI(I).LE.VARI(I+1))GO TO 97
  GO TO 1701
  M=-2
  C
  622 IF (I.NE.N)GO TO 1622
  I=N-2
  GO TO 802
  C
  COMPARE WITH NEXT
  1622 IF (VARI(I+1)-X)803,97,97
  803 I=1-1
  IF (I.EQ.1)GO TO 802
  C
  SEE WHICH THREE
  IF ((VARI(I-1)-X).LT.(X-VARI(I+2)))I=I-1
  802 IF (VARI(I).LE.VARI(I+1).OR.VARI(I+1).LE.VARI(I+2))GO TO 97
  GO TO 1702
  C
  M.GT.O
  31 DO 4 IYY=1,N
  I=IYY
  IF (X-VARI(I))700,119,4
  4 CONTINUE
  I=N-M
  C
  IF X.GT.X(N),EXTRAPCLATE

```

FTLU0010
 FTLU0020
 FTLU0030
 FTLU0040
 FTLU0050
 FTLU0060
 FTLU0070
 FTLU0080
 FTLU0090
 FTLU0100
 FTLU0110
 FTLU0120
 FTLU0130
 FTLU0140
 FTLU0150
 FTLU0160
 FTLU0170
 FTLU0180
 FTLU0190
 FTLU0200
 FTLU0210
 FTLU0220
 FTLU0230
 FTLU0240
 FTLU0250
 6TLU0270
 FTLU0280
 FTLU0290
 FTLU0300
 FTLU0310
 FTLU0320
 FTLU0330
 FTLU0340
 FTLU0350
 FTLU0360
 FTLU0370
 FTLU0380
 FTLU0390

APPENDIX - CONTINUED

ORIGINAL PAGE IS
OF POOR QUALITY

APPENDIX - CONTINUED

```

000137      IF(M.EQ.1)GO TO 701
000141      GO TO 702
          C      IF X.LT.X(1), EXTRAPOLATE
000141      700 IF(I.EQ.1.AND.M.EQ.1)GO TO 701
000150      IF(I.EQ.1.AND.M.EQ.2)GO TO 702
000155      IF(M.NE.1)GO TO 222
          C      M=1
000157      I=I-1
000160      701 IF(VARI(I+1).LE.VARI(I))GO TO 97
          C      LINEAR
000164      1701 Y=(VARD(I)*(VARI(I+1)-X)-VARD(I+1)*(VARI(I)-X))/(VARI(I+1)-VARI(I))
          C      RETURN
000177      RETURN
          C      M=2
000200      222 IF(I.NE.N)GO TO 1222
000202      I=N-2
000203      GO TO 702
          C      COMPARE WITH NEXT
000204      1222 IF(X-VARI(I+1))703,97,97
000207      703 I=I-1
000211      IF(I.EQ.1)GO TO 702
          C      SEE WHICH THREE
000212      IF(X-VARI(I-1)).LT.(VARI(I+2)-X))I=I-1
000220      702 IF(VARI(I+1).LE.VARI(I).OR.VARI(I+2).LE.VARI(I+1))GO TO 97
          C      SECOND ORDER
000233      1702 V(1)=VARI(I)-X
000235      V(2)=VARI(I+1)-X
000237      V(3)=VARI(I+2)-X
000241      K=I
000242      DO 704 J=1,2
000243      YY(J)=(VARD(K)*V(J+1)-VARD(K+1)*V(J))/(VARI(K+1)-VARI(K))
000257      704 K=K+1
000263      Y=(YY(1)*V(3)-YY(2)*V(1))/(VARI(I+2)-VARI(I))
000273      RETURN
          C      ZERO ORDER(Y=Y(I))
000274      1 Y=VARD(1)
000275      RETURN
          C      Y=Y(I)
000276      119 Y=VARD(I)
000300      RETURN
          C
          C      ERROR PRINT
000301      97 PRINT 103

```

FTLU0400
FTLU0410
FTLU0420
FTLU0430
FTLU0440
FTLU0450
FTLU0460
FTLU0470
FTLU0480
FTLU0490
FTLU0500
FTLU0510
FTLU0520
FTLU0530

FTLU0540

FTLU0560
FTLU0570
FTLU0580
FTLU0590
FTLU0600
FTLU0610
FTLU0620
FTLU0630
FTLU0640
FTLU0650
FTLU0660
FTLU0670
FTLU0680
FTLU0690
FTLU0700
FTLU0710
FTLU0720
FTLU0730
FTLU0740
FTLU0750
FTLU0760
FTLU0770
FTLU0780
FTLU0790

```

000305 103 FORMAT( /31H ERROR WAS ENCOUNTERED IN FTLUP)
000306 PRINT 1103,M,N,X
000323 1103 FORMAT( 1X,2HM=15,5X,2H=15,5X,2HX=E20.8)
000324 IF(N.EQ.0)STOP
000325 IF(M.EQ.0)STOP
000326 PRINT 1104
000341 1104 FORMAT( 19H TABLE OUT OF ORDER)
000342 STOP
000343 END

```

FTLU0800
 FTLU0810
 FTLU0820
 FTLU0830
 FTLU0840
 FTLU0850
 FTLU0860
 FTLU0870
 FTLU0880

APPENDIX - CONTINUED

ORIGINAL PAGE IS
OF POOR QUALITY

PROGRAM A4426 - WINDMILL EFFICIENCY ANALYSIS
CATENARY (N=2) - NEW AERODYNAMICS

APPENDIX - CONTINUED

ORIGINAL PAGE IS
OF POOR QUALITY

APPENDIX - CONTINUED

THETA	=	0.0,	0.5E+01,	0.1E+02,	0.15E+02,	0.2E+02,	0.25E+02,	0.3E+02,
		0.35E+02,	0.4E+02,	0.45E+02,	0.5E+02,	0.55E+02,	0.6E+02,	
		0.65E+02,	0.7E+02,	0.75E+02,	0.8E+02,	0.85E+02,	0.9E+02,	
		0.95E+02,	0.1E+03,	0.105E+03,	0.11E+03,	0.115E+03,	0.12E+03,	
		0.125E+03,	0.13E+03,	0.135E+03,	0.14E+03,	0.145E+03,	0.15E+03,	
		0.155E+03,	0.16E+03,	0.165E+03,	0.17E+03,	0.175E+03,	0.18E+03,	
		0.185E+03,	0.19E+03,	0.195E+03,	0.2E+03,	0.205E+03,	0.21E+03,	
		0.225E+03,	0.23E+03,	0.235E+03,	0.24E+03,	0.245E+03,	0.25E+03,	

APPENDIX - CONTINUED

APPENDIX - CONTINUED

ORIGINAL PAGE IS
OF POOR QUALITY

0.245E+03, 0.25E+03, 0.255E+03, 0.262E+03, 0.265E+03, 0.27E+03,
0.275E+03, 0.28E+03, 0.285E+03, 0.29E+03, 0.295E+03, 0.3E+03,
0.305E+03, 0.31E+03, 0.315E+03, 0.32E+03, 0.325E+03, 0.33E+03,
0.335E+03, 0.34E+03, 0.345E+03, 0.35E+03, 0.355E+03, 0.36E+03,
I, I, I, I, I, I, I, I, I, I, I, I, I, I, I, I,
I, I, I, I, I, I, I, I, I, I, I, I, I, I, I, I,
I, I, I, I, I, I, I, I, I, I, I, I, I, I, I, I,
I, I, I, I, I, I, I, I, I, I, I, I, I, I, I, I,
I, I, I, I, I, I, I, I, I, I, I, I, I, I, I, I,
I, I, I, I, I, I, I, I, I, I, I, I, I, I, I, I,

THPRNT = 0.0, I, I, I, I, I, I, I, I, I,

VRRY = 0.6E+01, 0.3E+01, 0.35E+01, 0.4E+01, 0.45E+01, 0.5E+01,
0.6E+01, 0.7E+01, 0.8E+01, 0.9E+01, 0.1E+02, 0.11E+02, I, I, I,
I, I, I, I, I,

YBAR = 0.0, 0.357E-01, 0.714E-01, 0.1071E+00, 0.1428E+00, 0.1785E+00,
0.2142E+00, 0.2499E+00, 0.2856E+00, 0.3213E+00, 0.357E+00,
0.3927E+00, 0.4284E+00, 0.4641E+00, 0.4998E+00, 0.5355E+00,
0.5712E+00, 0.6069E+00, 0.6426E+00, 0.6783E+00, 0.714E+00,
0.7497E+00, 0.7854E+00, 0.8211E+00, 0.8568E+00, 0.8925E+00,
0.9285E+00, 0.9639E+00, I, I, I, I, I, I, I, I, I, I,
I, I, I, I, I, I, I,

YMAX = 0.9639E+00,

YMIN = 0.0,

YSMAX = I,

YSMIN = I,

\$END

INPUT TABLES

GAMMA	CL	CC	CMC4	D/C
0.0000	0.	6.5000000E-02	0.	2.5000000E-01
2.0000	2.1000000E-01	6.0000000E-02	2.0000000E-03	2.4048305E-01
6.0000	6.9500000E-01	1.0000000E-02	6.0000000E-03	2.4133246E-01
8.0000	8.5300000E-01	1.2000000E-02	1.0000000E-02	2.3821240E-01
10.0000	9.6000000E-01	1.4000000E-02	2.0000000E-02	2.2889954E-01
12.0000	1.0150000E+00	4.5000000E-01	-3.5000000E-02	2.8492401E-01
12.7000	8.0000000E-01	1.0000000E-01	-6.5000000E-02	3.3100574E-01
14.0000	6.7000000E-01	1.7500000E-01	-7.0000000E-02	3.5109260E-01
16.0000	6.3000000E-01	2.1000000E-01	-7.2000000E-02	3.5851893E-01
18.0000	6.2000000E-01	2.4000000E-01	-7.6000000E-02	3.6287190E-01
20.0000	6.5500000E-01	2.4500000E-01	-8.0000000E-02	3.6440116E-01
30.0000	9.7500000E-01	5.9000000E-01	-1.6500000E-01	3.9481627E-01
40.0000	1.1300000E+00	9.7000000E-01	-2.6000000E-01	4.2459810E-01
42.0000	1.1390000E+00	1.0100000E+00	-2.7000000E-01	4.2736741E-01
50.0000	1.0900000E+00	1.3000000E+00	-3.3000000E-01	4.4451855E-01
60.0000	9.5900000E-01	1.5900000E+00	-3.9000000E-01	4.6007494E-01
70.0000	7.0000000E-01	1.8000000E+00	-4.3000000E-01	4.7269860E-01
80.0000	4.1000000E-01	1.9200000E+00	-4.8000000E-01	4.9464500E-01
90.0000	8.0000000E-02	1.9400000E+00	-5.2000000E-01	5.1804124E-01
100.0000	-2.2000000E-01	1.8900000E+00	-5.7000000E-01	5.5008067E-01
110.0000	-5.3300000E-01	1.7800000E+00	-5.9000000E-01	5.6806794E-01
120.0000	-7.9000000E-01	1.5700000E+00	-5.9500000E-01	5.8909706E-01
130.0000	-9.6000000E-01	1.3200000E+00	-5.8000000E-01	6.0620961E-01
140.0000	-1.0750000E+00	9.9000000E-01	-5.7000000E-01	6.4044907E-01
150.0000	-9.0000000E-01	6.0000000E-01	-4.7000000E-01	6.8541787E-01
155.0000	-7.2200000E-01	4.2000000E-01	-4.0000000E-01	7.3085367E-01
160.0000	-7.0300000E-01	2.8000000E-01	-3.4000000E-01	6.9840155E-01
164.0000	-7.5300000E-01	2.3000000E-01	-3.2000000E-01	6.5550001E-01
168.0000	-7.6100000E-01	1.9000000E-01	-3.5000000E-01	6.9650059E-01
170.0000	-7.6500000E-01	1.2000000E-01	-3.9000000E-01	7.5373558E-01
172.0000	-7.3000000E-01	8.0000000E-02	-4.2500000E-01	7.9240805E-01
180.0000	-1.0000000E-02	2.0000000E-02	-7.5000000E-02	7.7499999E+00

APPENDIX - CONTINUED

OUTPUT

NONDIMENSIONAL WINDMILL SWEEP AREA SBAR= 2.7700361E+00

APPENDIX - CONTINUED

ORIGINAL PAGE IS
OF POOR QUALITY

VELOCITY RATIO RMAX*OMEGA/VINF = 6.0000

WINDMILL THRUST COEFFICIENT BARCT = 7.9552433E-01

VR = 7.4803774E-01

ITERATIONS = 3

THETA = 0.00

WINDMILL BLADE LIFT, DRAG AND MOMENT

YBAR	GAMMA	CL	CD	D/C	DEL CM
0.	7.11	6.8646994E-01	1.6463737E-02	2.3960619E-01	1.5326166E-01
1.0000000E-02	7.12	6.8706981E-01	1.6481662E-02	2.3955283E-01	1.5305275E-01
2.0000000E-02	7.12	6.8755414E-01	1.6499131E-02	2.3957983E-01	1.5283925E-01
3.0000000E-02	7.13	6.8822286E-01	1.6516141E-02	2.3956717E-01	1.5262121E-01
4.0000000E-02	7.14	6.8861646E-01	1.6527917E-02	2.3955841E-01	1.5243195E-01
5.0000000E-02	7.14	6.8874146E-01	1.6531657E-02	2.3955563E-01	1.5227137E-01
6.0000000E-02	7.14	6.8879260E-01	1.6533188E-02	2.3955449E-01	1.5209097E-01
7.0000000E-02	7.14	6.8876977E-01	1.6532505E-02	2.3955500E-01	1.5189081E-01
8.0000000E-02	7.14	6.8876426E-01	1.6532340E-02	2.3955512E-01	1.5154327E-01
9.0000000E-02	7.14	6.8863344E-01	1.6528425E-02	2.3955803E-01	1.5113793E-01
1.0000000E-01	7.13	6.8835715E-01	1.6520158E-02	2.3956418E-01	1.5069444E-01
1.1000000E-01	7.13	6.8802397E-01	1.6510191E-02	2.3957160E-01	1.5018074E-01
1.2000000E-01	7.12	6.8775992E-01	1.6502294E-02	2.3957747E-01	1.4954992E-01
1.3000000E-01	7.12	6.8734569E-01	1.6489098E-02	2.3958669E-01	1.4888106E-01
1.4000000E-01	7.11	6.8678084E-01	1.6473026E-02	2.3959927E-01	1.4817446E-01
1.5000000E-01	7.11	6.8640328E-01	1.6461745E-02	2.3960767E-01	1.4738181E-01
1.6000000E-01	7.10	6.8602769E-01	1.6450527E-02	2.3961603E-01	1.4653904E-01
1.7000000E-01	7.09	6.8552547E-01	1.6435531E-02	2.3962721E-01	1.4566634E-01
1.8000000E-01	7.09	6.8496678E-01	1.6418855E-02	2.3963964E-01	1.4472817E-01
1.9000000E-01	7.08	6.8467069E-01	1.6410021E-02	2.3964623E-01	1.4355554E-01
2.0000000E-01	7.07	6.8422790E-01	1.6396812E-02	2.3965609E-01	1.4235104E-01
2.1000000E-01	7.07	6.8363726E-01	1.6379204E-02	2.3966923E-01	1.4111523E-01
2.2000000E-01	7.06	6.8316907E-01	1.6365247E-02	2.3967965E-01	1.3991650E-01
2.3000000E-01	7.05	6.8278577E-01	1.6352826E-02	2.3968819E-01	1.3874489E-01
2.4000000E-01	7.05	6.8230065E-01	1.6339376E-02	2.3969898E-01	1.3755388E-01
2.5000000E-01	7.04	6.8171351E-01	1.6321895E-02	2.3971205E-01	1.3634223E-01
2.6000000E-01	7.03	6.8106309E-01	1.6302539E-02	2.3972653E-01	1.3494982E-01
2.7000000E-01	7.02	6.8028664E-01	1.6279444E-02	2.3974381E-01	1.3353569E-01
2.8000000E-01	7.01	6.7938312E-01	1.6252598E-02	2.3976392E-01	1.3210036E-01
2.9000000E-01	6.99	6.7858604E-01	1.6228911E-02	2.3978166E-01	1.3062481E-01
3.0000000E-01	6.99	6.7797180E-01	1.6210674E-02	2.3979533E-01	1.2910724E-01
3.1000000E-01	6.97	6.7724602E-01	1.6189138E-02	2.3981149E-01	1.2757431E-01
3.2000000E-01	6.96	6.7640759E-01	1.6164273E-02	2.3983015E-01	1.2602654E-01
3.3000000E-01	6.96	6.7556509E-01	1.6151157E-02	2.3984000E-01	1.2442896E-01
3.4000000E-01	6.95	6.7530184E-01	1.6137431E-02	2.3985031E-01	1.2281598E-01

APPENDIX - CONTINUED

APPENDIX - CONTINUED

ORIGINAL PAGE IS
OF POOR QUALITY

3.5000000E-01	6.94	6.7454135E-01	1.6120844E-02	2.3987162F-01	1.0211777E-01	1.1956992E-01
3.6000000E-01	6.94	6.7454427E-01	1.6109072E-02	2.3986864E-01	1.1796013E-01	1.1796013E-01
3.7000000E-01	6.94	6.7467802E-01	1.6113032E-02	2.3986711E-01	1.1634733E-01	1.1634733E-01
3.8000000E-01	6.94	6.7474651E-01	1.6115071E-02	2.3987704E-01	1.1473191E-01	1.1473191E-01
3.9000000E-01	6.94	6.7475000E-01	1.6115163E-02	2.3987789E-01	1.1302178E-01	1.1302178E-01
4.0000000E-01	6.93	6.7426276E-01	1.6110739E-02	2.3989435E-01	1.1127288E-01	1.1127288E-01
4.1000000E-01	6.92	6.7352303E-01	1.6078851E-02	2.3991308E-01	1.0951950E-01	1.0951950E-01
4.2000000E-01	6.91	6.7268169E-01	1.6053572E-02	2.3992913E-01	1.0770796E-01	1.0770796E-01
4.3000000E-01	6.90	6.7196026E-01	1.6032651E-02	2.3992117E-01	1.0561232E-01	1.0561232E-01
4.4000000E-01	6.90	6.7231915E-01	1.6042226E-02	2.3991505E-01	1.0352056E-01	1.0352056E-01
4.5000000E-01	6.91	6.7259283E-01	1.6051345E-02	2.3991083E-01	1.0143338E-01	1.0143338E-01
4.6000000E-01	6.91	6.7278254E-01	1.6056953E-02	2.3990854E-01	9.9438463E-02	9.9438463E-02
4.7000000E-01	6.91	6.7288565E-01	1.6060003E-02	2.3990799E-01	9.7509286E-02	9.7509286E-02
4.8000000E-01	6.91	6.7291024E-01	1.6060729E-02	2.3990918E-01	9.5585775E-02	9.5585775E-02
4.9000000E-01	6.91	6.7295657E-01	1.6059154E-02	2.3991170E-01	9.3665923E-02	9.3665923E-02
5.0000000E-01	6.91	6.7274357E-01	1.6055801E-02	2.3989467E-01	9.1630049E-02	9.1630049E-02
5.1000000E-01	6.92	6.7350865E-01	1.6078426E-02	2.3987884E-01	8.9605271E-02	8.9605271E-02
5.2000000E-01	6.93	6.7421973E-01	1.6099466E-02	2.3986425E-01	8.7592139E-02	8.7592139E-02
5.3000000E-01	6.94	6.7487559E-01	1.6118882E-02	2.3983312E-01	8.5542070E-02	8.5542070E-02
5.4000000E-01	6.95	6.7552494E-01	1.6139004E-02	2.3981844E-01	8.3445990E-02	8.3445990E-02
5.5000000E-01	6.96	6.7627408E-01	1.6160316E-02	2.3980511E-01	8.1365030E-02	8.1365030E-02
5.6000000E-01	6.97	6.7693377E-01	1.6175876E-02	2.3976675E-01	7.9299796E-02	7.9299796E-02
5.7000000E-01	6.98	6.7753251E-01	1.6197637E-02	2.3972503E-01	7.7182164E-02	7.7182164E-02
5.8000000E-01	7.00	6.7925600E-01	1.6248911E-02	2.3968346E-01	7.5075422E-02	7.5075422E-02
5.9000000E-01	7.03	6.8113062E-01	1.6304548E-02	2.3964076E-01	7.2989712E-02	7.2989712E-02
6.0000000E-01	7.06	6.8239826E-01	1.6360157E-02	2.3959530E-01	7.0894001E-02	7.0894001E-02
6.1000000E-01	7.08	6.8491666E-01	1.6417360E-02	2.3950440E-01	6.8751681E-02	6.8751681E-02
6.2000000E-01	7.11	6.8695924E-01	1.6479357E-02	2.3942448E-01	6.6634477E-02	6.6634477E-02
6.3000000E-01	7.14	6.8900100E-01	1.6539425E-02	2.39323014E-01	6.4542997E-02	6.4542997E-02
6.4000000E-01	7.17	6.9142397E-01	1.6600594E-02	2.3923294E-01	6.2380629E-02	6.2380629E-02
6.5000000E-01	7.22	6.9463361E-01	1.6708386E-02	2.3913347E-01	6.0215318E-02	6.0215318E-02
6.6000000E-01	7.28	6.9887251E-01	1.6836014E-02	2.3892297E-01	5.8082460E-02	5.8082460E-02
6.7000000E-01	7.35	7.0223969E-01	1.6967533E-02	2.3882760E-01	5.5998356E-02	5.5998356E-02
6.8000000E-01	7.41	7.0770854E-01	1.7103372E-02	2.3903484E-01	5.4022851E-02	5.4022851E-02
6.9000000E-01	7.47	7.1213975E-01	1.7238118E-02	2.3892297E-01	5.2078568E-02	5.2078568E-02
7.0000000E-01	7.54	7.1671672E-01	1.7377785E-02	2.3866695E-01	5.0156014E-02	5.0156014E-02
7.1000000E-01	7.61	7.2145082E-01	1.7522707E-02	2.3846233E-01	4.8147363E-02	4.8147363E-02
7.2000000E-01	7.71	7.2966856E-01	1.7744672E-02	2.3824568E-01	4.6075795E-02	4.6075795E-02
7.3000000E-01	7.84	7.3786223E-01	1.8029116E-02	2.3762694E-01	4.4045816E-02	4.4045816E-02
7.4000000E-01	7.98	7.4759597E-01	1.8332362E-02	2.3694520E-01	4.1892227E-02	4.1892227E-02
7.5000000E-01	8.13	7.5487440E-01	1.8603746E-02	2.3622037E-01	3.9824768E-02	3.9824768E-02
7.6000000E-01	8.27	7.6160872E-01	1.8866252E-02	2.3544781E-01	3.7810262E-02	3.7810262E-02
7.7000000E-01	8.43	7.6876864E-01	1.9146479E-02	2.3456896E-01	3.5849235E-02	3.5849235E-02
7.8000000E-01	8.59	7.7640009E-01	1.9446445E-02	2.3355764E-01	3.3887832E-02	3.3887832E-02
7.9000000E-01	8.78	7.8508152E-01	1.9789291E-02	2.3246317E-01	3.1922301E-02	3.1922301E-02
8.0000000E-01	9.00	7.9507145E-01	2.0185933E-02	2.3127428E-01	3.0019143E-02	3.0019143E-02
8.1000000E-01	9.23	8.0588271E-01	2.0617741E-02	2.3127428E-01	2.8179172E-02	2.8179172E-02
8.2000000E-01	9.49	8.1762677E-01	2.1089817E-02	2.3018754E-01	2.6694403E-02	2.6694403E-02
8.3000000E-01	9.72	8.2836171E-01	2.1524074E-02	2.2904319E-01	2.5289692E-02	2.5289692E-02
8.4000000E-01	9.97	8.3966576E-01	2.1984184E-02	2.27866602E-01	2.3153613E-02	2.3153613E-02
8.5000000E-01	10.23	8.5133444E-01	2.25786602E-02			

8.600000E-01	10.58	8.5501959E-01	3.1275466E-02	2.4510079E-01	2.0770636E-02
8.700000E-01	11.09	8.6729783E-01	3.9414774E-02	2.5937601E-01	1.8037579E-02
8.800000E-01	11.66	8.8119455E-01	4.8631107E-02	2.7553294E-01	1.5564121E-02
8.900000E-01	12.32	8.0237090E-01	7.7692354E-02	3.0618319E-01	9.7762153E-03
9.000000E-01	13.04	6.7152648E-01	1.2447126E-01	3.3618675E-01	3.2272296E-03
9.100000E-01	13.84	6.0107442E-01	1.6984401E-01	3.4861168E-01	-4.6723255E-04
9.200000E-01	14.77	5.7344616E-01	1.9228175E-01	3.5396625E-01	-1.3067786E-03
9.300000E-01	15.95	5.5288122E-01	2.1255684E-01	3.5832411E-01	-1.5528604E-03
9.400000E-01	17.88	5.5196186E-01	2.4159121E-01	3.6260024E-01	-1.3516103E-03
9.500000E-01	20.37	5.8424162E-01	2.6164926E-01	3.6552686E-01	-5.1262216E-04
9.600000E-01	23.71	6.7790231E-01	3.7824765E-01	3.7568767E-01	-7.5695022E-04
9.639000E-01	25.34	7.2347547E-01	4.3505390E-01	3.8063168E-01	-7.4488488E-04

CM(0.0)= 8.6899397E-02

APPENDIX - CONTINUED

FLYNN (FLETA)

APPENDIX - CONTINUED

240.00	2.2619901E-03	0.
245.00	-2.6298138E-03	0.
250.00	-6.4796958E-03	0.
255.00	-8.9284351E-03	0.
260.00	-1.0147028E-02	0.
265.00	-1.0171479E-02	0.
270.00	-9.9691143E-03	0.
275.00	-7.6369365E-03	0.
280.00	-5.0513613E-03	0.
285.00	-1.2599894E-03	0.
290.00	3.7920792E-03	0.
295.00	1.0353570E-02	0.
300.00	1.7814015E-02	0.
305.00	2.5962460E-02	0.
310.00	3.4555551E-02	0.
315.00	4.3373375E-02	0.
320.00	5.2117018E-02	0.
325.00	6.0507098E-02	0.
330.00	6.8282991E-02	0.
335.00	7.4915154E-02	0.
340.00	7.9567621E-02	0.
345.00	8.3063335E-02	0.
350.00	8.5477176E-02	0.
355.00	8.6758499E-02	0.
360.00	8.689397E-02	0.

APPENDIX - CONTINUED

NUMBER OF BLADES = 2

CMTS

THETA CMT

0.00	1.4651683E-01	0.
5.00	1.4498248E-01	0.
10.00	1.4134564E-01	0.
15.00	1.3573144E-01	0.
20.00	1.282501E-01	0.
25.00	1.1900776E-01	0.
30.00	1.0757342E-01	0.
35.00	9.4780477E-02	0.
40.00	8.0917816E-02	0.
45.00	6.5784310E-02	0.
50.00	5.0699422E-02	0.
55.00	3.5217730E-02	0.
60.00	2.2791238E-02	0.
65.00	1.0866548E-02	0.
70.00	8.4469570E-04	0.
75.00	-6.7409507E-03	0.
80.00	-1.1583473E-02	0.
85.00	-1.355109E-02	0.
90.00	-1.3871558E-02	0.
95.00	-1.3267817E-02	0.
100.00	-1.0228123E-02	0.
105.00	-4.8007454E-03	0.
110.00	3.2678120E-03	0.
115.00	1.3909992E-02	0.
120.00	2.6354452E-02	0.
125.00	4.0193874E-02	0.
130.00	5.4965070E-02	0.
135.00	7.020909E-02	0.
140.00	8.5372540E-02	0.
145.00	9.9329351E-02	0.
150.00	1.1212209E-01	0.
155.00	1.2327214E-01	0.
160.00	1.3182251E-01	0.
165.00	1.3842510E-01	0.
170.00	1.4322226E-01	0.
175.00	1.4592927E-01	0.

APPENDIX - CONCLUDED

AVERAGE BLADE MOMENT COEFFICIENT, CMA = 6.2614295E-02
AVERAGE STRUT MOMENT COEFFICIENT, CMAS = 0.

POWER COEFFICIENT WITHOUT NONLIFTING STRUT LOSSES, CPA = 3.7568577E-01
POWER LOST DUE TO NONLIFTING STRUTS, CPL = 0.
NET POWER COEFFICIENT, CPN = 3.7568577E-01

Table I. Aerodynamic Characteristic of the
NACA 0012 Airfoil at Reynolds Numbers
of $.5 \times 10^6$ and 1.8×10^6

α , degrees	C_L	C_D	$C_{M_{c/4}}$	d/c	Rey
0.0000	0.	6.5000000E-03	0.	2.5000000E-01	
2.0000	2.1000000E-01	8.0000000E-03	2.0000000E-03	2.4048305E-01	
6.0000	6.9300000E-01	1.0000000E-02	6.0000000E-03	2.4133246E-01	
8.0000	8.5300000E-01	1.2000000E-02	1.0000000E-02	2.3821240E-01	
10.0000	9.6000000E-01	1.4000000E-02	2.0000000E-02	2.2889954E-01	$.5 \times 10^6$
12.0000	1.0150000E+00	4.5000000E-02	-3.5000000E-02	2.8492401E-01	
12.7000	8.0000000E-01	1.0000000E-01	-6.5000000E-02	3.3100574E-01	
14.0000	6.7000000E-01	1.7500000E-01	-7.0000000E-02	3.5109260E-01	
16.0000	6.3000000E-01	2.1000000E-01	-7.2000000E-02	3.5851893E-01	
18.0000	6.3000000E-01	2.4000000E-01	-7.6000000E-02	3.6287190E-01	
20.0000	6.5500000E-01	2.4500000E-01	-8.0000000E-02	3.6440116E-01	
30.0000	9.7500000E-01	5.9000000E-01	-1.6500000E-01	3.9481627E-01	
40.0000	1.1300000E+00	9.7000000E-01	-2.6000000E-01	4.2459810E-01	
42.0000	1.1390000E+00	1.0100000E+00	-2.7000000E-01	4.2736741E-01	
50.0000	1.0900000E+00	1.3000000E+00	-3.3000000E-01	4.4451855E-01	1.8×10^6
60.0000	9.5900000E-01	1.5900000E+00	-3.9000000E-01	4.6007494E-01	
70.0000	7.0000000E-01	1.8000000E+00	-4.3000000E-01	4.7269860E-01	
80.0000	4.1000000E-01	1.9200000E+00	-4.8000000E-01	4.9464500E-01	
90.0000	8.0000000E-02	1.9400000E+00	-5.2000000E-01	5.1804124E-01	
100.0000	-2.2000000E-01	1.9900000E+00	-5.7000000E-01	5.5008067E-01	
110.0000	-5.3300000E-01	1.7800000E+00	-5.9000000E-01	5.6806794E-01	
120.0000	-7.9000000E-01	1.5700000E+00	-5.9500000E-01	5.8909706E-01	
130.0000	-9.6000000E-01	1.3200000E+00	-5.8000000E-01	6.0620961E-01	
140.0000	-1.0750000E+00	9.9000000E-01	-5.7000000E-01	6.4044907E-01	
150.0000	-9.0000000E-01	6.0000000E-01	-4.7000000E-01	6.8541787E-01	
155.0000	-7.2200000E-01	4.2000000E-01	-4.0000000E-01	7.3085367E-01	
160.0000	-7.0300000E-01	2.8000000E-01	-3.4000000E-01	6.5840155E-01	
164.0000	-7.5300000E-01	2.3000000E-01	-3.2000000E-01	6.5550001E-01	
169.0000	-7.6100000E-01	1.9000000E-01	-3.5000000E-01	6.9650059E-01	
170.0000	-7.6300000E-01	1.2000000E-01	-3.9000000E-01	7.5273558E-01	
172.0000	-7.3000000E-01	8.0000000E-02	-4.2500000E-01	7.9240805E-01	
180.0000	-1.0000000E-02	2.0000000E-02	-7.5000000E-02	7.7499959E+00	

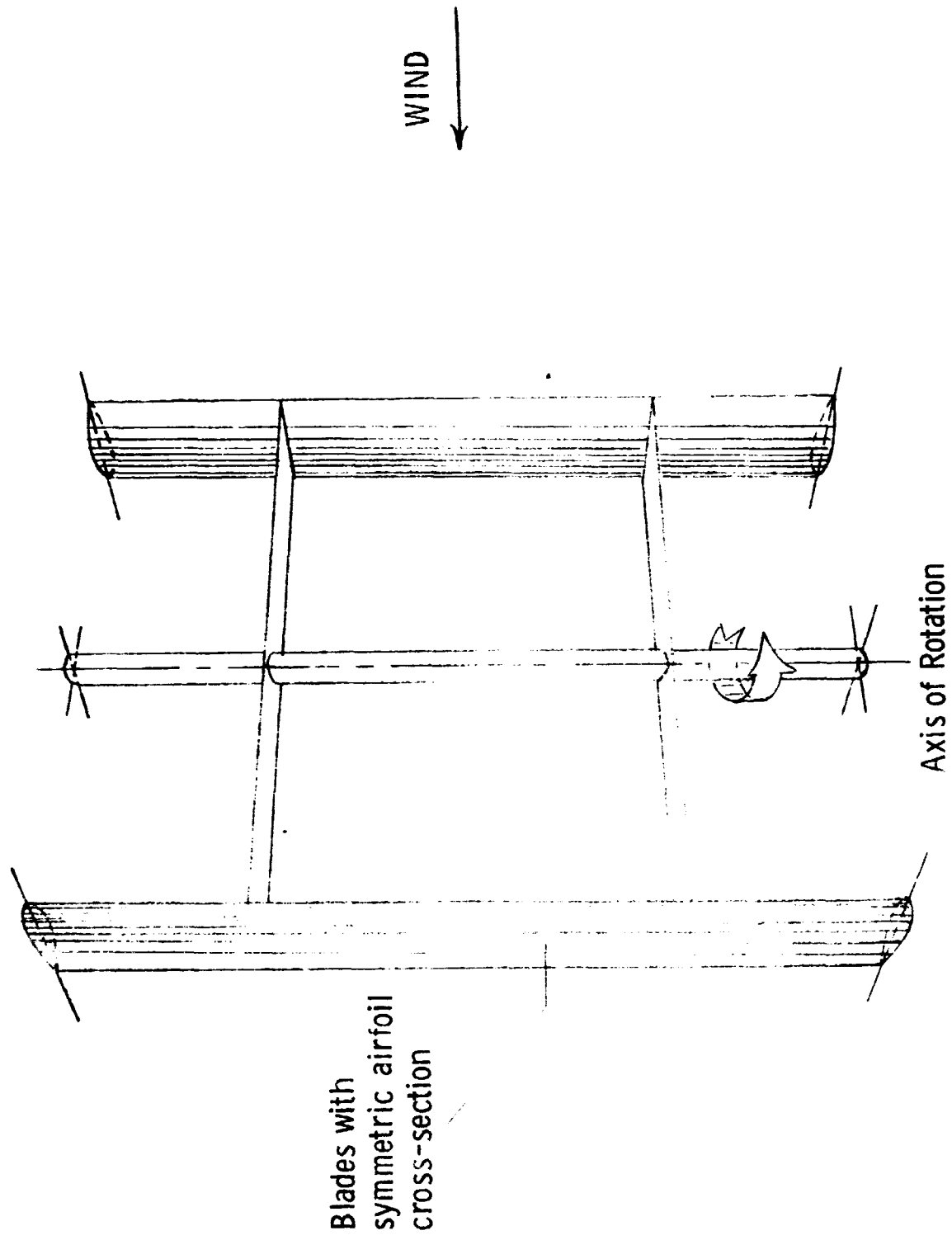


Figure 1. The Vertical Axis Windmill.

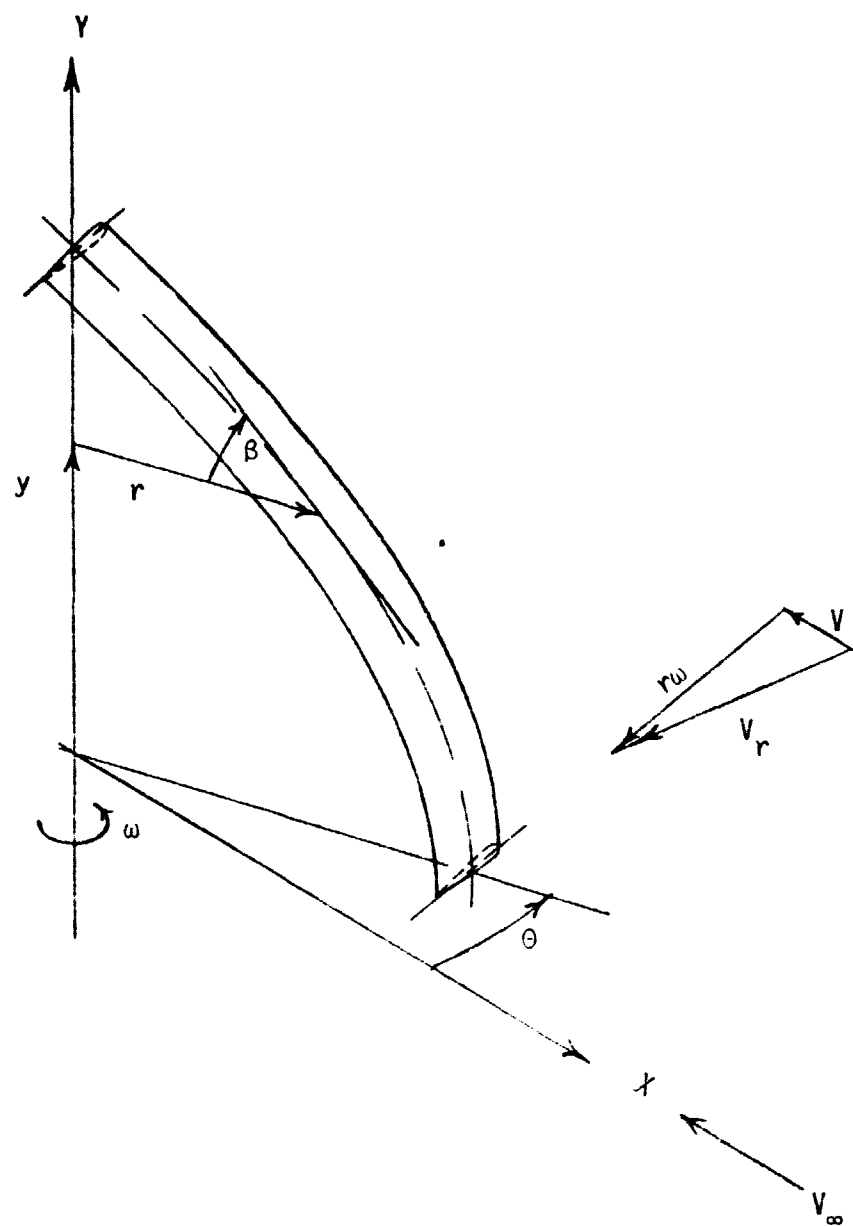
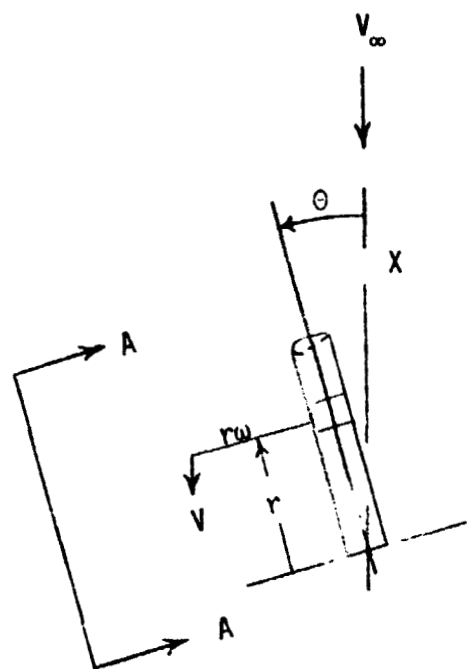


FIGURE 2 - Coordinate System.



Windmill blade viewed from above.

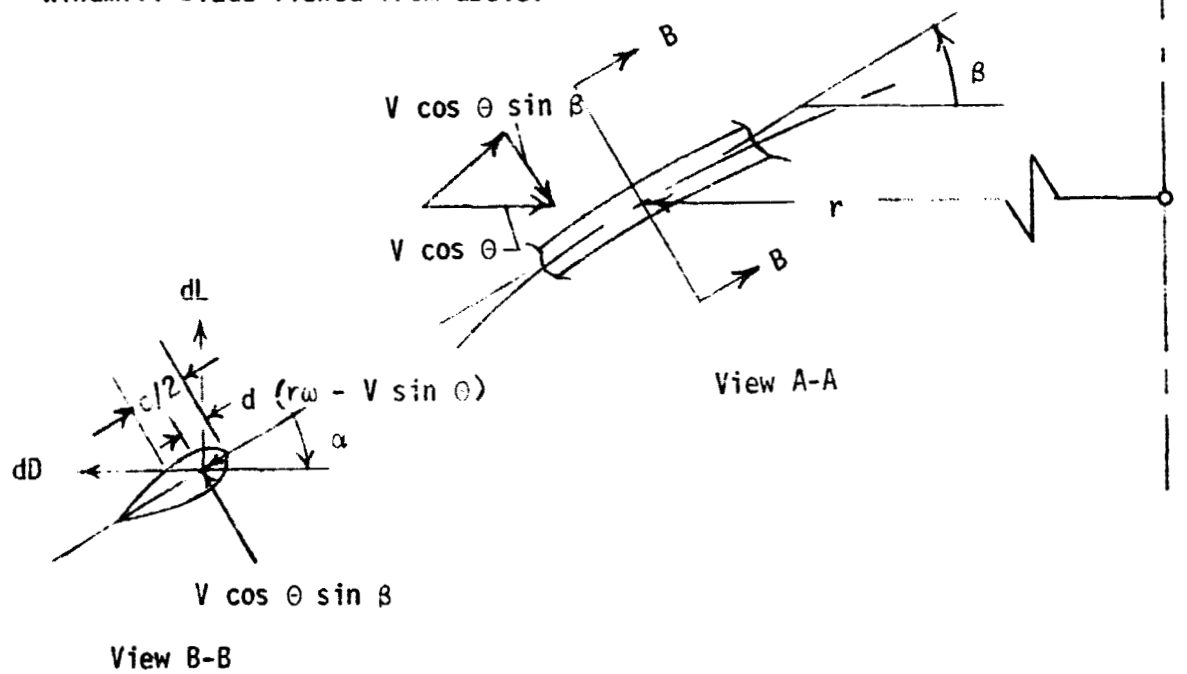


Figure 3. - Velocity and force vector components.

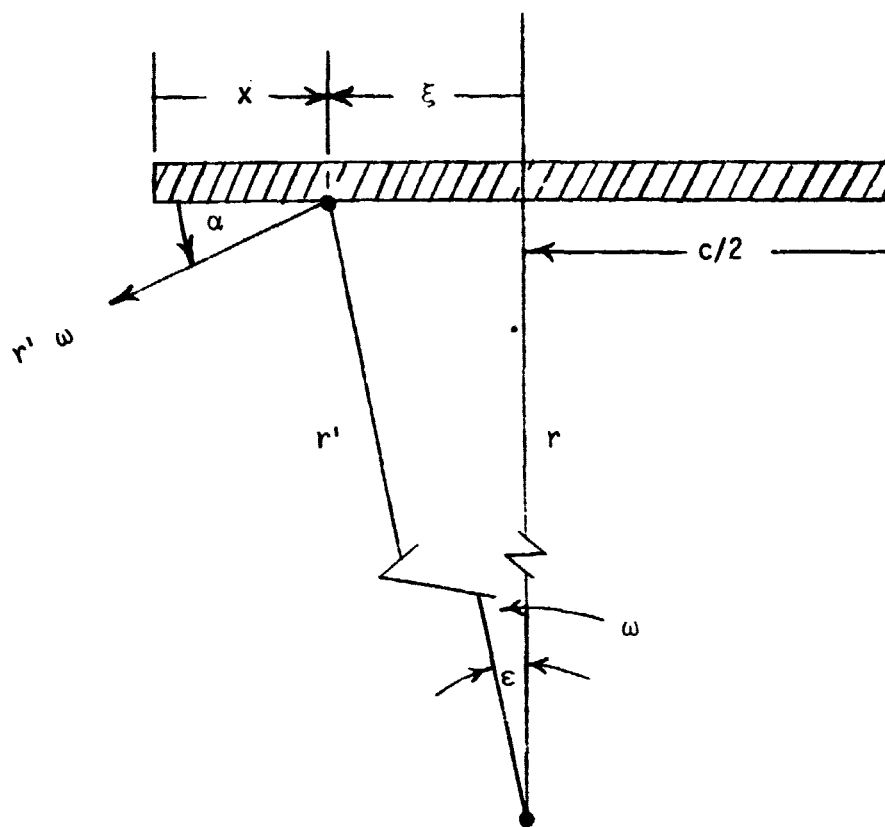


FIGURE 4. - Local Coordinates for Flow Curvature Analysis.

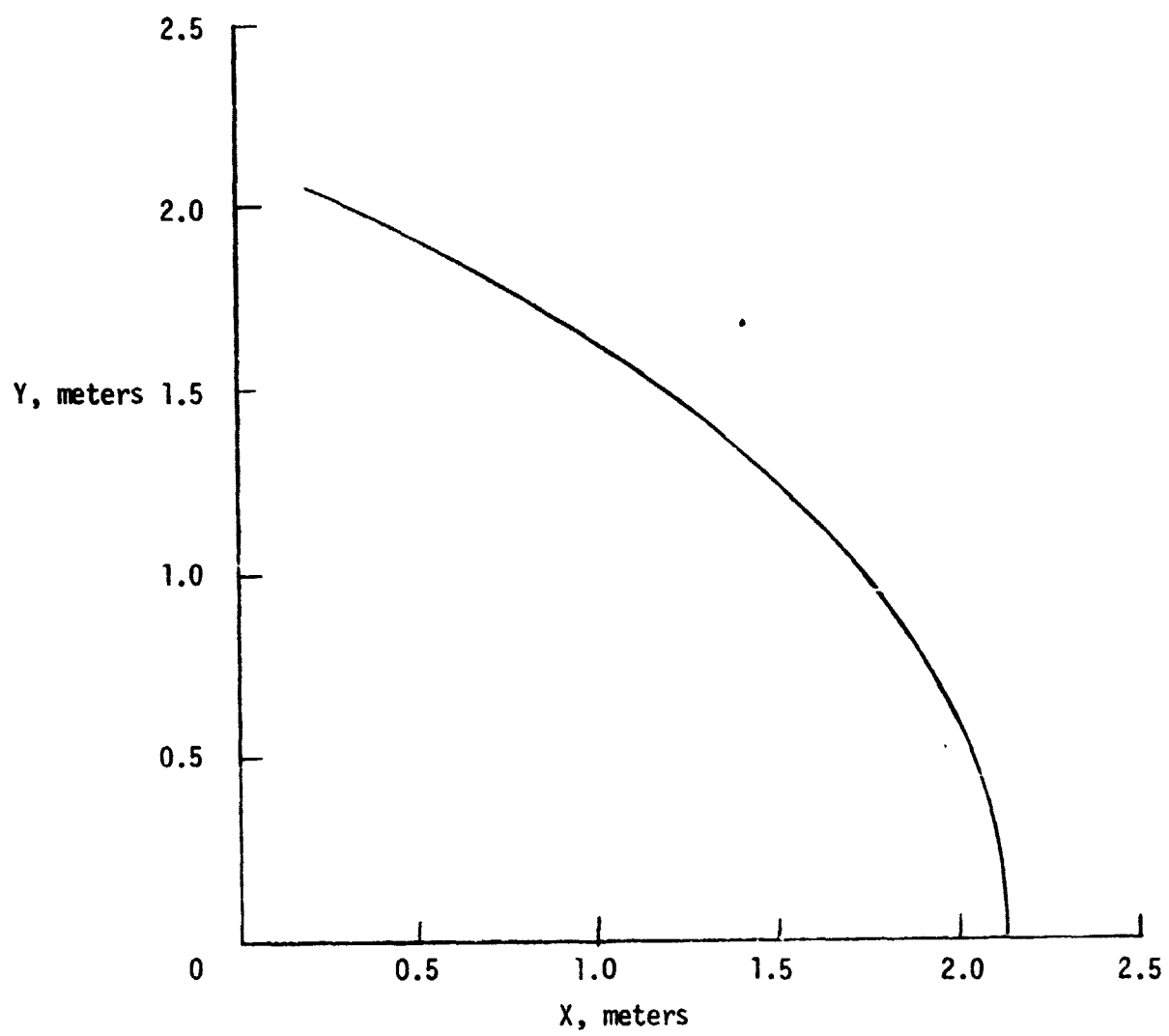


Figure 5. - Side View of the Upper Half of a Blade.

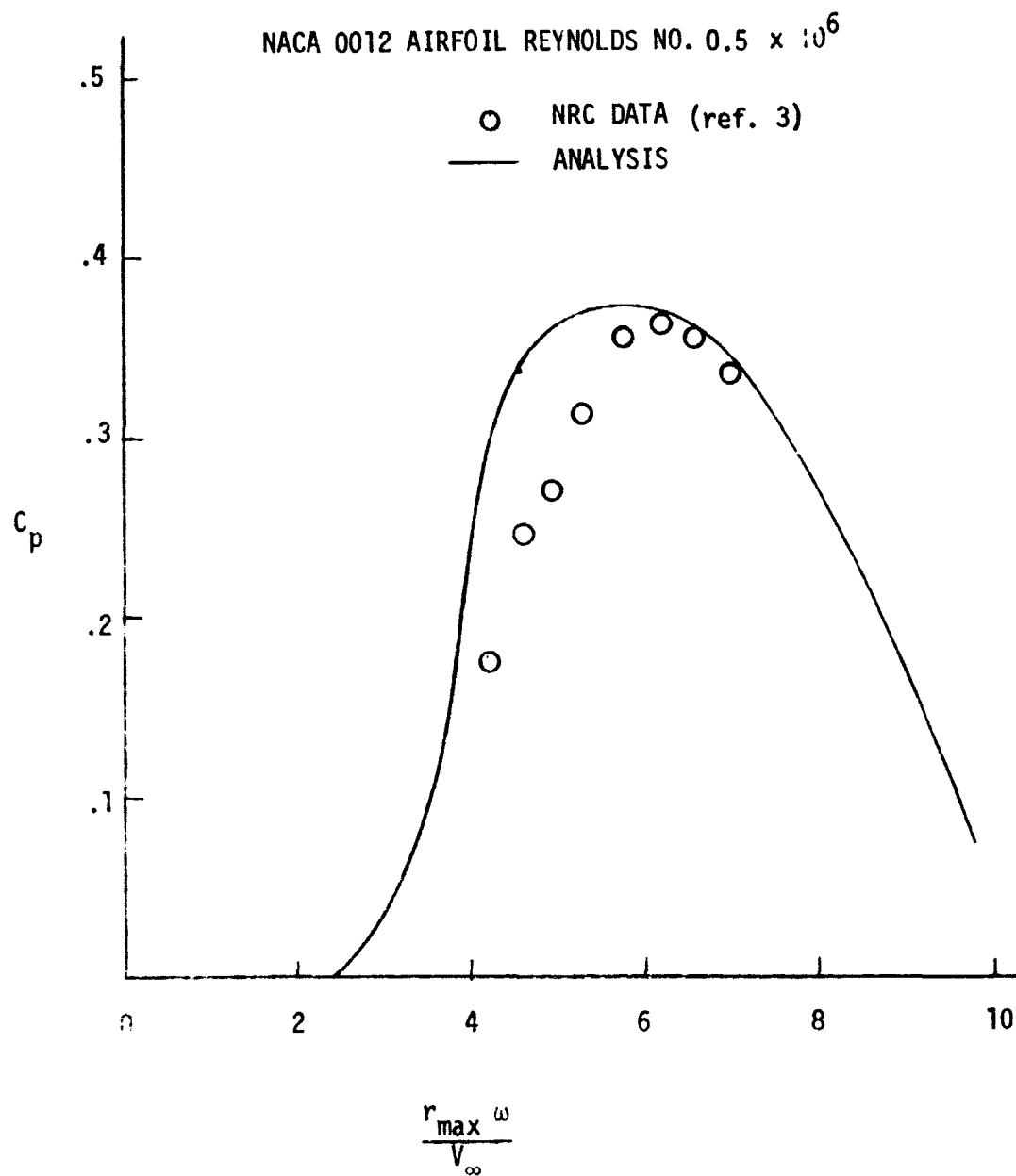


FIGURE 6. - Comparison of Analysis with Test Data for a Two Blade Catenary VAW Using the NACA 0012 Airfoil.

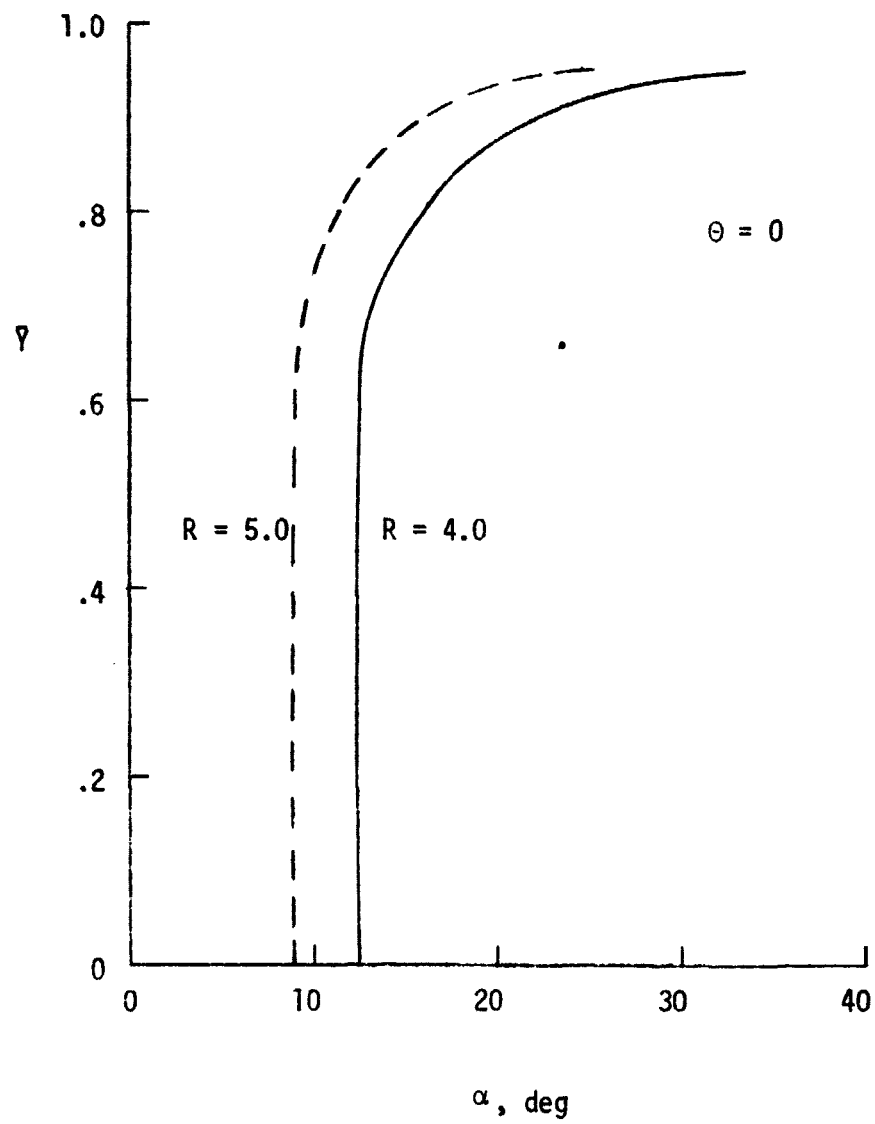


FIGURE 7 - Variation of Angle of Attack Along the Blade - Catenary VAW.

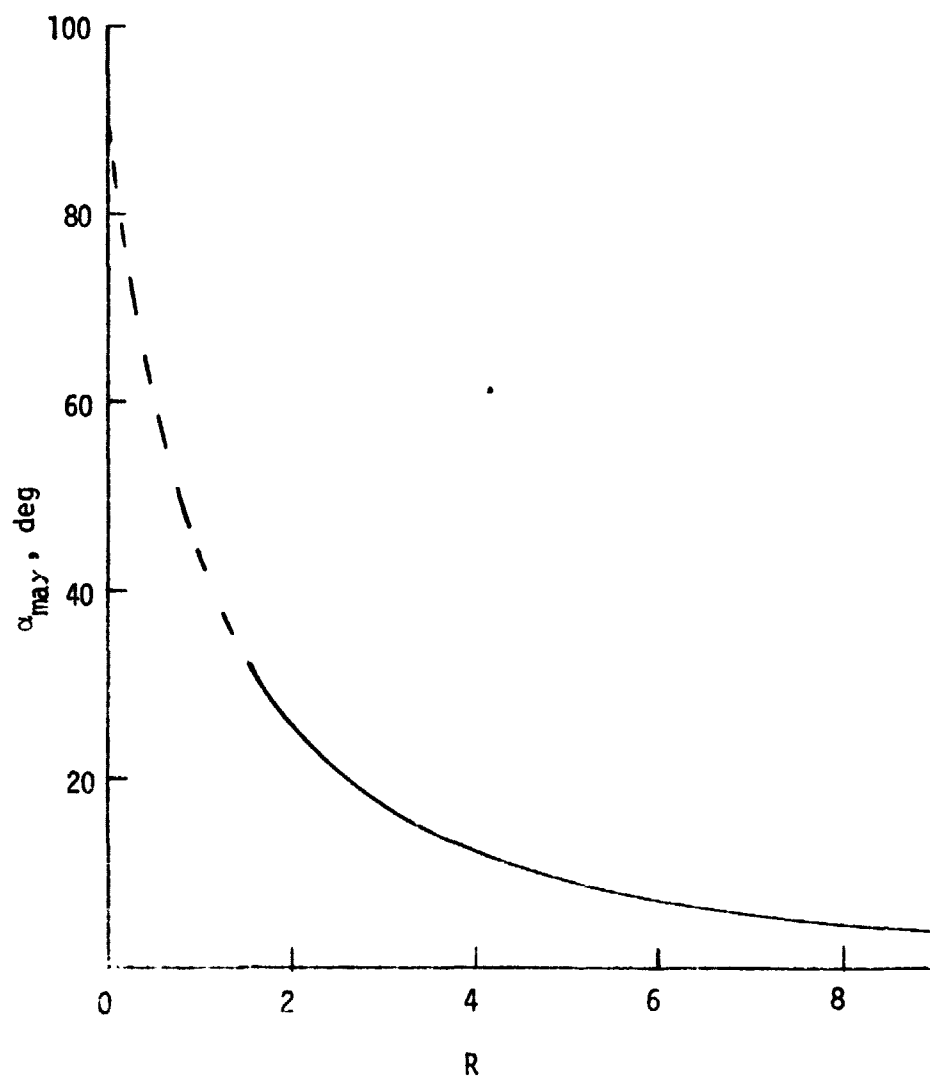


FIGURE 8 - Maximum Angle of Attack Envelope for the Catenary VAW as a Function of R .

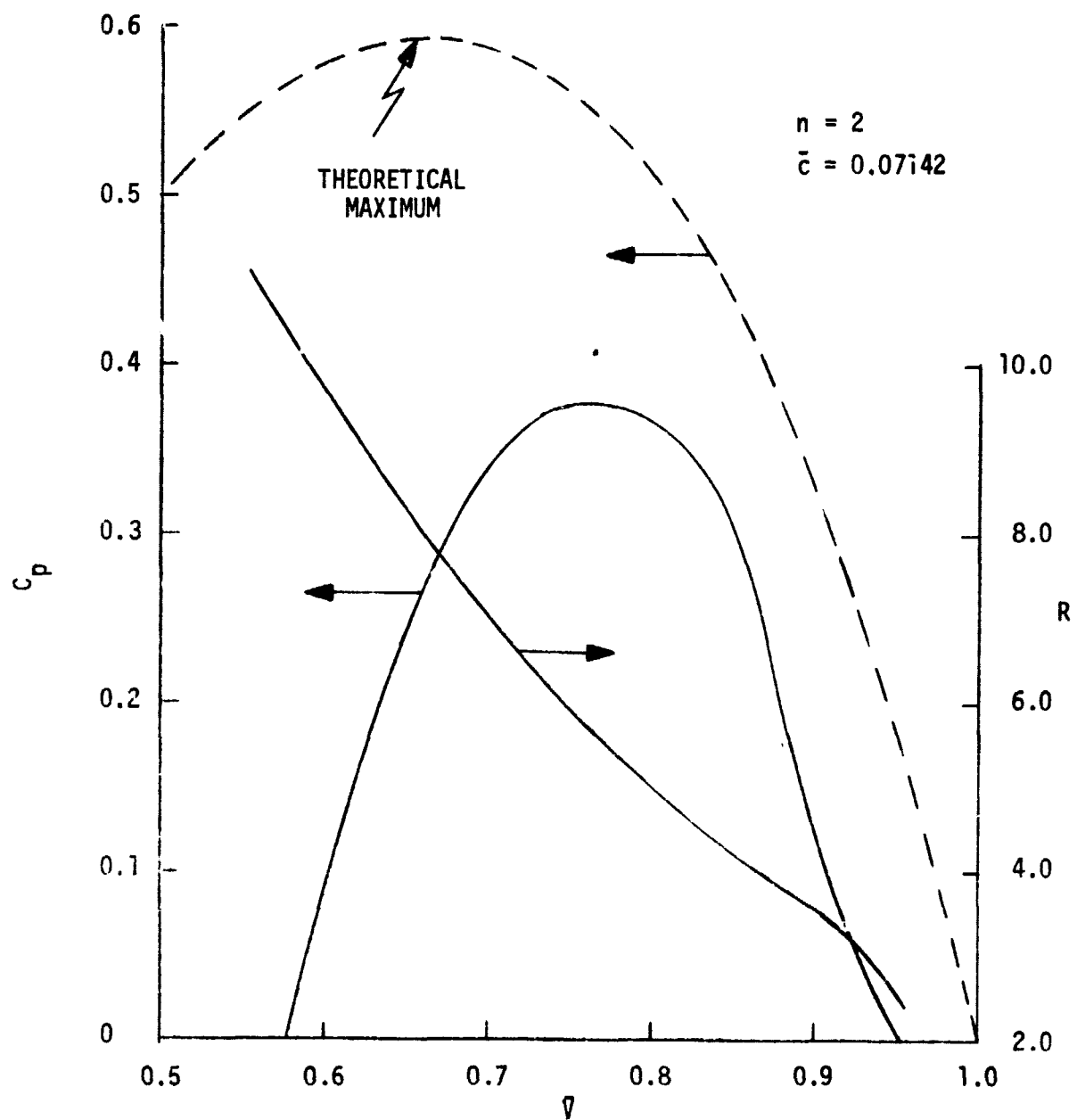


FIGURE 9 - Performance Characteristics of the Catenary Windmill.

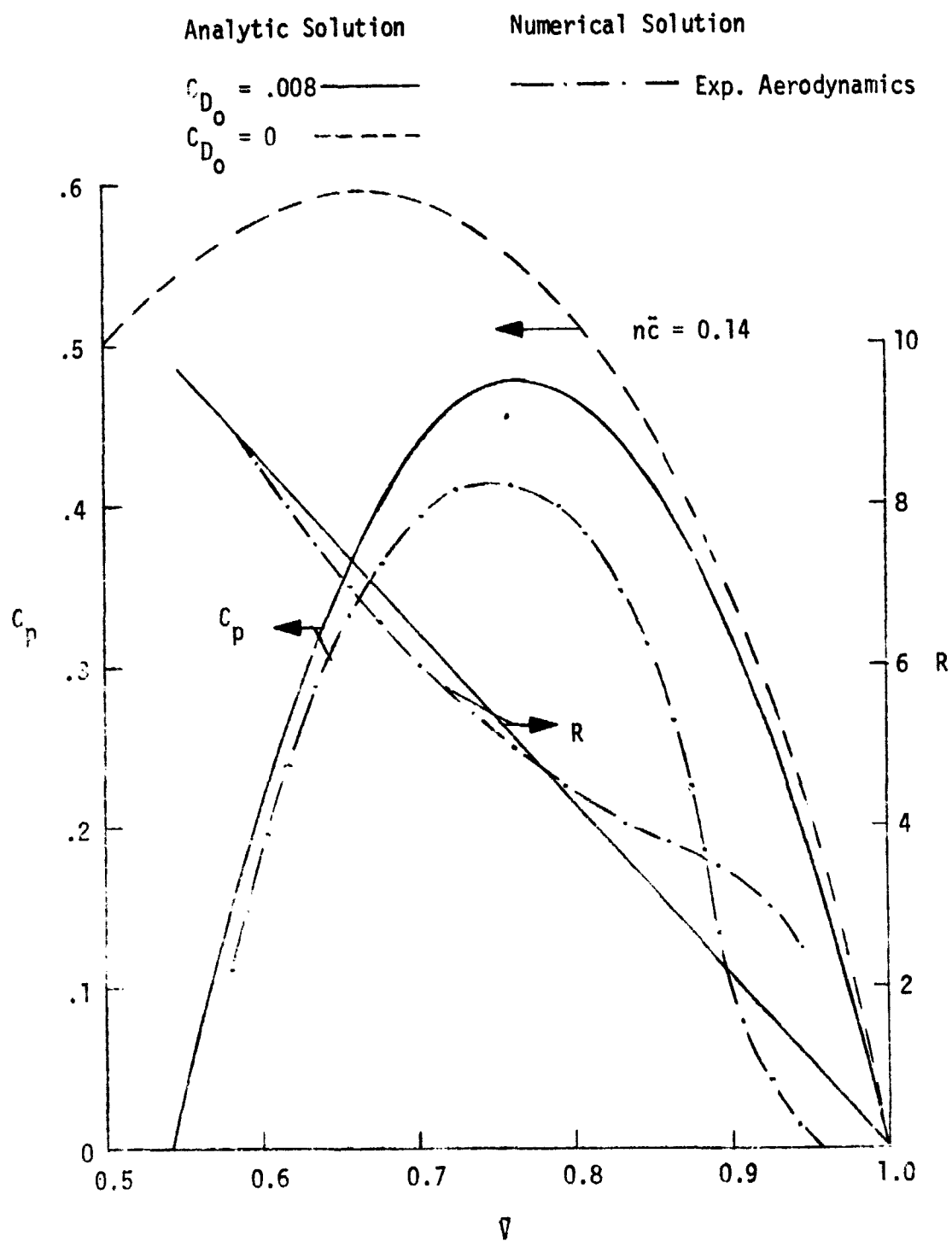


FIGURE 10 - Performance Characteristics of a Straight Blade VAW.

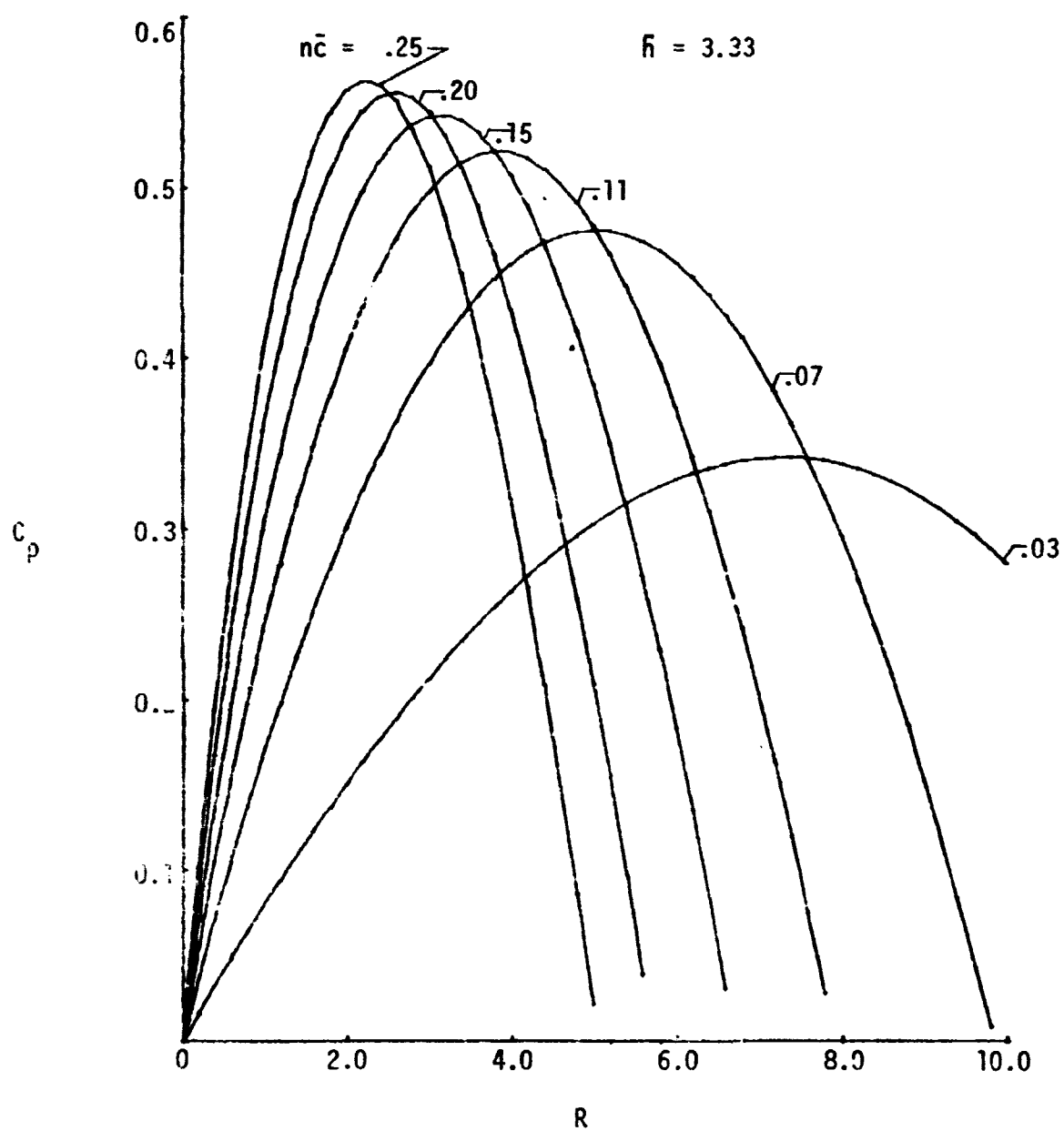


FIGURE 11 - Effect of Solidity on the Performance of a Straight Blade VAW - Analytical Solution.

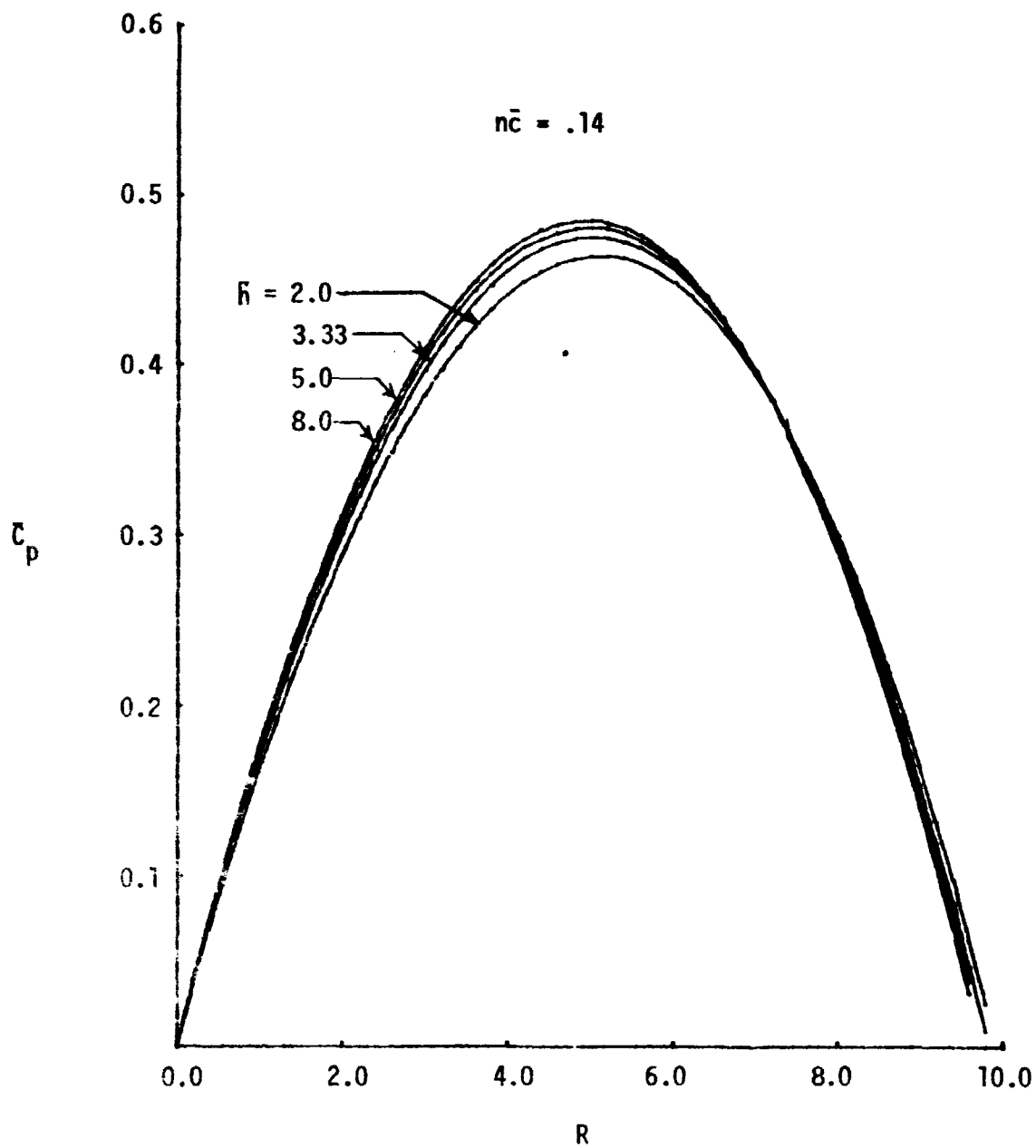


FIGURE 12 - Effect of Windmill Aspect Ratio \bar{H} on Performance for a Straight Blade Design - Analytical Results.

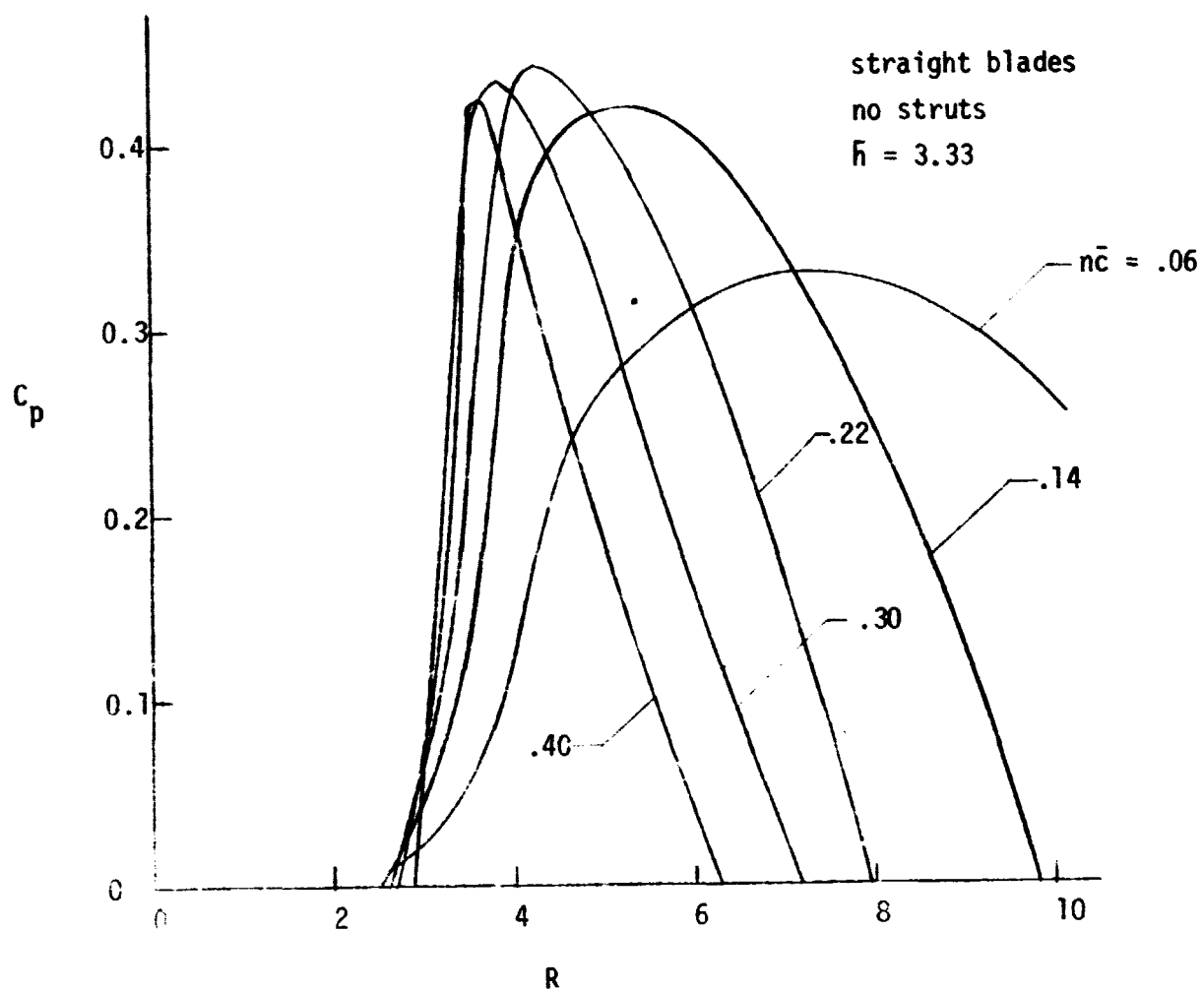
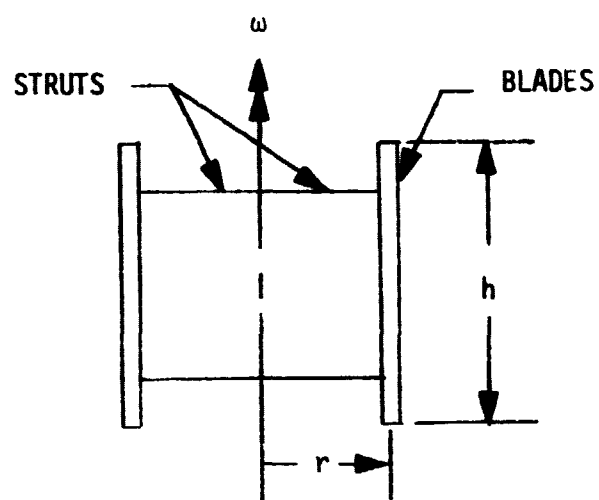
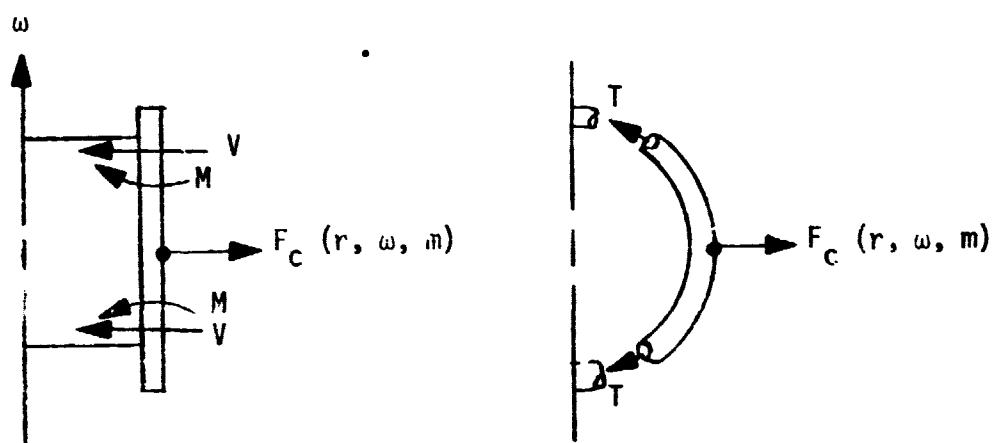


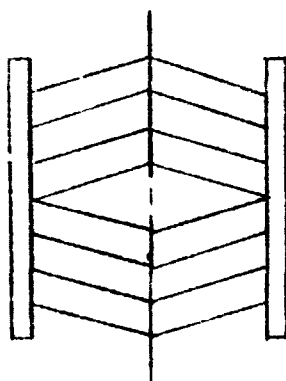
FIGURE 13 - Effect of Solidity on Performance for a Straight Blade Configuration - Numerical Results.



a) STRAIGHT BLADE CONFIGURATION.



b) TYPICAL LOADING FOR STRAIGHT AND CURVED BLADE VAW.



c) CHEVRON STRAIGHT BLADE VAW CONCEPT.

FIGURE 14 - Straight and Curved Blade VAW Designs.

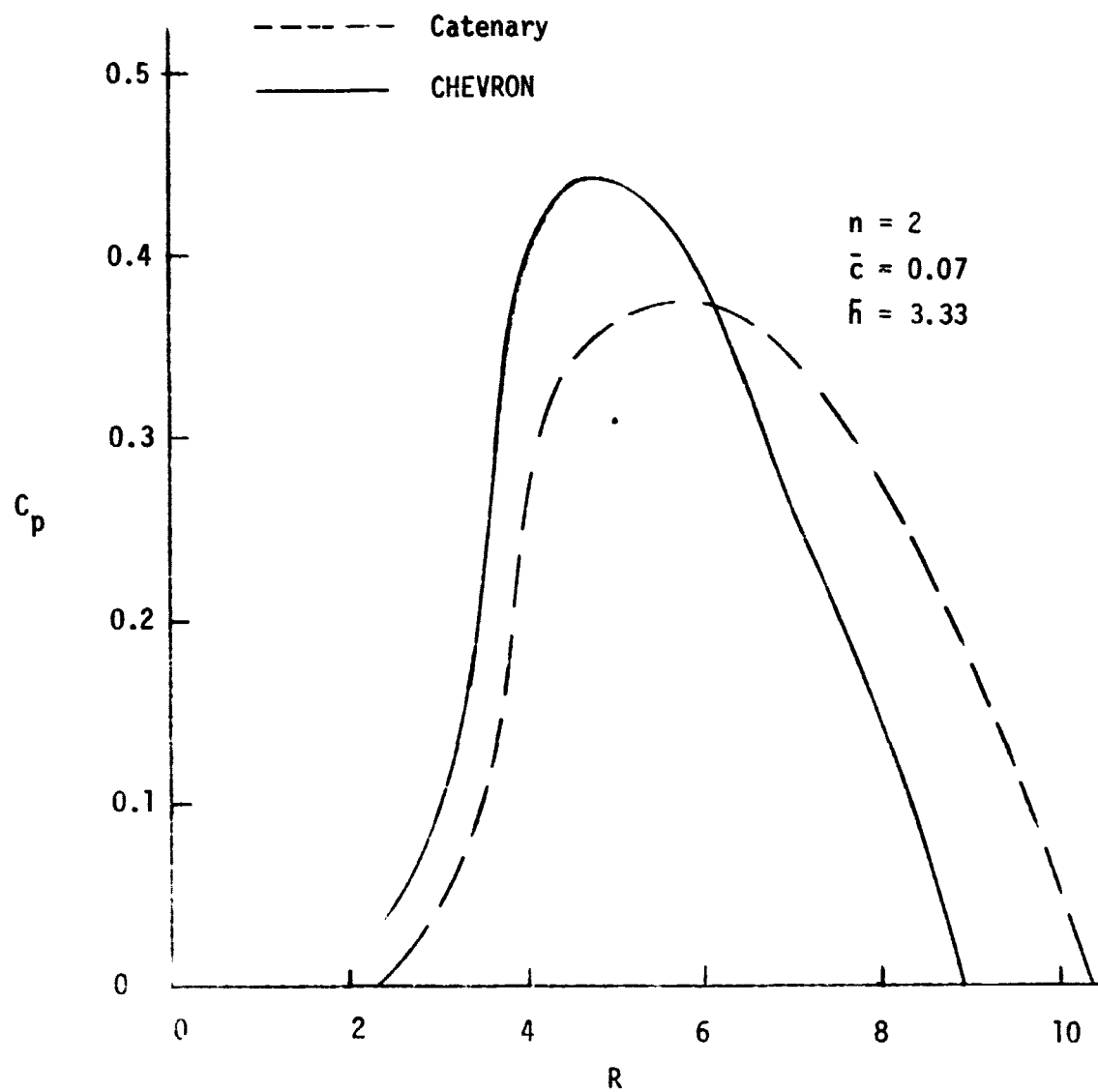


FIGURE 15 - Performance Characteristics of a Chevron Type Straight Blade VAW.